J. Fluid Mech. (1980), *vol.* 96, *part* 3, *pp.* 417–445
Printed in Great Britain

Some effects of surface tension on steep water waves. Part 2

By S. J. HOGAN
Department of Applied Mathematics and Theoretical Physics,
University of Cambridge, Silver Street, Cambridge CB3 9EW†

(Received 2 February 1979)

This paper continues an investigation of the effects of surface tension on steep water waves in deep water begun in Hogan (1979*a*). A Stokes-type expansion method is given which can be applied to most wavelengths. For capillary waves (2 cm or less) it is found that the surface of the highest wave encloses a bubble of air, as was found for pure capillary waves by Crapper (1957). For intermediate waves (20 cm) the wave profiles are similar to those of pure gravity waves and the wave properties increase monotonically. For gravity waves (200 cm) the wave properties all exhibit a maximum just short of the maximum wave height obtained by the method. The integral properties for all the waves are drawn and given in numerical form in the appendix.

1. Introduction

In a recent paper (Hogan 1979*a*, hereinafter referred to as I) some results of work on pure capillary waves were presented. Exact expressions were obtained for the wave energy and flux of momentum, energy and mass of the wave in terms of the wave amplitude. It was also proved that the potential energy is always greater than the kinetic energy. In addition it was found that the crest height of such waves, when referred to the mean level, is not a monotonic function of wave height.

In the present paper, using methods pioneered by Stokes (1880), and developed by Schwartz (1974) and Longuet-Higgins (1975), we consider waves with both gravity and surface tension taken into account. No exact solutions were found but, using a computer to perform the algebra, very accurate results can be obtained. We find that for short wavelengths the wave is very capillary-like in nature. The highest wave bends over and touches itself, enclosing a bubble of air. The crest height above the mean level is not a monotonic function of wave height and the potential energy exceeds the kinetic energy. In addition the gravitational potential energy is greatest at a height short of the maximum. For intermediate waves where surface tension is not quite so important, the wave properties are monotonic in the wave amplitude. We find that the wave trough broadens and the wave crest narrows as the amplitude increases, the phase speed and other integral properties increase and the total kinetic energy exceeds the total potential energy. However, for gravity waves the present method reveals the existence of a wave of greatest energy at a height less than the maximum obtained by this method. In fact all the properties of these gravity waves

† Present address: Applied Mathematics Department 101–50, California Institute of Technology, Pasadena, California 91125.

are not monotonic functions of wave height. The case of waves in which the present method breaks down, the so-called Wilton ripples, is to be included in a further paper. In § 2, we set up the problem and derive the governing equations. In § 3 the perturbation solution is given. In § 4 we quote the results and § 5 is devoted to a discussion of their consequences.

2. The governing equations for gravity–capillary waves

We develop a method for analysing symmetric two-dimensional periodic gravity–capillary waves on the surface of an ideal fluid of infinite depth. We have at our disposal two limiting cases against which our results can be checked. Pure gravity waves have been analysed by Schwartz (1972, 1974), Longuet-Higgins (1975) and Cokelet (1977), pure capillary waves by Crapper (1957) and I. However it was Wilton (1915) who presented the first significant results for the general problem and it is with this paper that most comparison will be made. With a suitable choice of reference frame, the waves can be brought to rest with the fluid at great depths moving to the left with the phase speed c. We choose axes with y vertically upwards, and x horizontal and to the right. We assume irrotationality of the flow and an inviscid incompressible fluid. In addition, as in I, we take the mean level as the line $y = 0$ and the mean horizontal velocity as zero.

Following Stokes (1880) we consider the velocity potential Φ and stream function Ψ (both relative to the moving reference frame) as independent variables. In fact the notation is the same as in I, with in addition the wavelength λ normalized to 2π and the acceleration due to gravity to 1, although we will change this later on.

Let

$$\Phi + i\Psi = -ic\ln W \tag{2.1}$$

so

$$W = \exp(i\Phi/c) \quad \text{on the free surface} \quad y = \eta \quad (\text{where } \Psi = 0),$$

$$W \to 0 \quad \text{as} \quad y \to -\infty \quad (\text{where } \Psi \sim -cy).$$

In general

$$x + iy = i\left(\ln W + \sum_{n=0}^{\infty} \frac{1}{n} a_n W^n\right), \tag{2.2}$$

where the a_n $(n = 0, 1, 2, \ldots)$ are all real. a_0 does not have the same value as in I but serves the same purpose, that is of fixing the origin of y. The particle velocity (U, v) is given by

$$U - iv = \frac{d(\Phi + i\Psi)}{d(x+iy)} = \frac{-c}{\left(1 + \sum_{n=1}^{\infty} a_n W^n\right)}.$$

At the free surface $y = \eta$, Bernoulli's condition can be written as

$$|U_s - iv_s|^2 + 2(\eta - a_0) - \frac{2\tau\eta''}{(1+\eta'^2)^{\frac{3}{2}}} = K, \tag{2.3}$$

where the subscript s denotes surface values, τ is the surface tension divided by the density, the prime denotes d/dx and K is a constant. If we put $\Psi = 0$ in (2.2) and equate real and imaginary parts we obtain

$$x = -\Phi/c - \sum_{n=1}^{\infty} \frac{a_n}{n} \sin\left(\frac{n\Phi}{c}\right) \equiv f(\Phi/c), \tag{2.4a}$$

$$\eta = a_0 + \sum_{n=1}^{\infty} \frac{a_n}{n} \cos\left(\frac{n\Phi}{c}\right) \equiv g(\Phi/c), \tag{2.4b}$$

where, from now on, everything is considered to be evaluated at the surface.

The curvature can then be rewritten as

$$\frac{\eta''}{(1+\eta'^2)^{\frac{3}{2}}} = \frac{\dot{f}\ddot{g}-\dot{g}\ddot{f}}{(\dot{f}^2+\dot{g}^2)^{\frac{3}{2}}} \tag{2.5}$$

where the dot denotes $d/d(\Phi/c)$. Then making use of the identity

$$x_\Phi^2 + \eta_\Phi^2 = \frac{1}{U_s^2+v_s^2},$$

we see that

$$c^2(x_\Phi^2+\eta_\Phi^2) = \dot{f}^2+\dot{g}^2 = \left|1+\sum_{n=1}^{\infty} a_n W^n\right|^2. \tag{2.6}$$

Equations (2.5) and (2.6) enable us to write equation (2.3) in the following form:

$$c^2+[2(\eta-a_0)-K]\left[\left|1+\sum_{n=1}^{\infty} a_n W^n\right|^2\right] = 2\tau(\dot{f}\ddot{g}-\dot{g}\ddot{f})\Big/\left|1+\sum_{n=1}^{\infty} a_n W^n\right|. \tag{2.7}$$

We then substitute equations (2.4*a*, *b*) into equation (2.7) and equate coefficients of $\cos(n\Phi/c)$. However, this is rather complicated to do all at once so we break down the calculation into smaller pieces.

Write

$$\dot{f}\ddot{g}-\dot{g}\ddot{f} = \sum_{k=0}^{\infty} q_k \cos\left(\frac{k\Phi}{c}\right), \tag{2.8a}$$

$$\left|1+\sum_{n=1}^{\infty} a_n W^n\right| = -\sum_{k=0}^{\infty} u_k \cos\left(\frac{k\Phi}{c}\right), \tag{2.8b}$$

$$\frac{\dot{f}\ddot{g}-\dot{g}\ddot{f}}{\left|1+\sum_{n=1}^{\infty} a_n W^n\right|} = -\sum_{k=0}^{\infty} w_k \cos\left(\frac{k\Phi}{c}\right), \tag{2.8c}$$

$$c^2+[2(\eta-a_0)-K]\left[\left|1+\sum_{n=1}^{\infty} a_n W^n\right|^2\right] = \sum_{k=0}^{\infty} s_k \cos\left(\frac{k\Phi}{c}\right). \tag{2.8d}$$

We have chosen the negative sign in equation (2.8*b*), following Wilton, that is, we take the radius of curvature to be positive in the wave troughs.

From equation (2.7) we must then solve

$$s_n = -2\kappa w_n, \quad n = 0, 1, 2, \ldots. \tag{2.9}$$

κ is a non-dimensional number arising naturally in the problem; in general it is given by $\kappa = 4\pi^2\tau/\lambda^2 g$. The s_n $(n = 0, 1, 2, \ldots)$ can be expressed in terms of c^2, K, a_0, a_1, ... as follows:

$$s_0 = c^2 + 2\sum_{k=1}^{\infty} \frac{a_k f_k}{k} - Kf_0, \tag{2.10a}$$

$$\tfrac{1}{2}s_n = \sum_{k=1}^{\infty} \frac{a_k}{k}(f_{|k-n|} + f_{n+k}) - Kf_n, \quad n = 1, 2, \ldots, \tag{2.10b}$$

where

$$f_0 = 1 + \sum_{k=1}^{\infty} a_k^2, \tag{2.11a}$$

$$f_n = a_n + \sum_{k=1}^{\infty} a_k a_{k+n}, \quad n = 1, 2, \ldots. \tag{2.11b}$$

We note that if $\tau = 0$ then equation (2.9) implies that $s_n = 0$ $(n = 0, 1, 2, \ldots)$. In this case equations (2.10a, b) are exactly equations (2.6a, b) of Schwartz (1974), evaluated at infinite depth.

3. The perturbation solution

Following Schwartz we let ϵ be a global parameter associated with the wave height which vanishes with the wave height. Then we assume power series expansions in terms of ϵ of each of the $a_j, f_j, q_j, s_j, u_j, w_j, c^2$ and K. Thus

$$a_j = \sum_{k=0}^{\infty} \alpha_{jk}\epsilon^{j+2k}, \quad j = 1, 2, \ldots, \tag{3.1a}$$

$$f_j = \sum_{k=0}^{\infty} \beta_{jk}\epsilon^{j+2k}, \quad j = 0, 1, \ldots, \tag{3.1b}$$

$$q_j = \sum_{k=0}^{\infty} \mu_{jk}\epsilon^{j+2k}, \quad j = 0, 1, \ldots, \tag{3.1c}$$

$$s_j = \sum_{k=0}^{\infty} \sigma_{jk}\epsilon^{j+2k}, \quad j = 0, 1, \ldots, \tag{3.1d}$$

$$u_j = \sum_{k=0}^{\infty} \tau_{jk}\epsilon^{j+2k}, \quad j = 0, 1, \ldots, \tag{3.1e}$$

$$w_j = \sum_{k=0}^{\infty} \zeta_{jk}\epsilon^{j+2k}, \quad j = 0, 1, \ldots, \tag{3.1f}$$

$$c^2 = \sum_{k=0}^{\infty} \gamma_k\epsilon^{2k}, \tag{3.1g}$$

$$K = \sum_{k=0}^{\infty} \delta_k\epsilon^{2k}. \tag{3.1h}$$

We then substitute equations (3.1) into equations (2.8), (2.9), (2.10) and (2.11) and equate coefficients of ϵ. The following recurrence relations are then obtained:

$$\sigma_{0k} = \gamma_k + 2\sum_{r=0}^{k-1} \frac{1}{k-r}\sum_{m=0}^{r} \alpha_{k-r,r-m}\beta_{k-r,m} - \sum_{p=0}^{k} \delta_{k-p}\beta_{0p}, \quad k = 0, 1, \ldots; \tag{3.2a}$$

$$\tfrac{1}{2}\sigma_{jk} = \sum_{l=1}^{j} \frac{1}{l} \sum_{s=0}^{k} \alpha_{l,k-s}\beta_{j-l,s} + \sum_{l=1}^{k} \frac{1}{l+j} \sum_{s=0}^{k-l} \alpha_{l+j,k-l-s}\beta_{ls}$$
$$+ \sum_{l=0}^{k-1} \frac{1}{k-l} \sum_{s=0}^{l} \alpha_{k-l,l-s}\beta_{j+k-l,s} - \sum_{l=0}^{k} \delta_l \beta_{j,k-l}, \quad j = 1,2,\ldots \text{ and } k = 0,1,\ldots; \tag{3.2b}$$

$$\beta_{00} = 1, \quad \beta_{0k} = \sum_{l=1}^{k} \sum_{r=0}^{k-l} \alpha_{lr}\alpha_{l,k-l-r}, \quad k = 1,2,\ldots; \tag{3.2c}$$

$$\beta_{jk} = \alpha_{jk} + \sum_{l=1}^{k} \sum_{r=0}^{k-l} \alpha_{lr}\alpha_{l+j,k-l-r}, \quad j = 1,2,\ldots \text{ and } k = 0,1,\ldots; \tag{3.2d}$$

$$\beta_{0k} = \sum_{l=0}^{k} \tau_{0l}\tau_{0,k-l} + \frac{1}{2}\sum_{l=1}^{k} \sum_{m=0}^{k-l} \tau_{lm}\tau_{l,k-l-m}, \quad k = 0,1,\ldots; \tag{3.2e}$$

$$\beta_{jk} = \sum_{l=0}^{k} \tau_{jl}\tau_{0,k-l} + \frac{1}{2}\sum_{l=1}^{k} \sum_{m=0}^{k-l} \tau_{lm}\tau_{j+l,k-l-m}$$
$$+ \frac{1}{4}\sum_{l=1}^{j-1} \sum_{m=0}^{k} \tau_{l,k-m}\tau_{j-l,m}, \quad j = 1,2,\ldots \text{ and } k = 0,1,\ldots; \tag{3.2f}$$

$$\mu_{00} = 0, \quad \mu_{0k} = \sum_{l=0}^{k-1} (k-l) \sum_{m=0}^{l} \alpha_{k-l,l-m}\alpha_{k-l,m}, \quad k = 1,2,\ldots; \tag{3.2g}$$

$$\mu_{jk} = j\alpha_{jk} + \sum_{m=1}^{k} (j+2m) \sum_{p=0}^{k-m} \alpha_{mp}\alpha_{j+m,k-m-p}, \quad j = 1,2,\ldots \text{ and } k = 0,1,\ldots; \tag{3.2h}$$

$$\mu_{0k} = \sum_{l=0}^{k} \zeta_{0l}\tau_{0,k-l} + \frac{1}{2}\sum_{l=1}^{k} \sum_{m=0}^{k-l} \zeta_{lm}\tau_{l,k-l-m}, \quad k = 0,1,\ldots; \tag{3.2j}$$

$$\mu_{jk} = \sum_{l=0}^{k} (\zeta_{jl}\tau_{0,k-l} + \zeta_{0l}\tau_{j,k-l}) + \frac{1}{2}\sum_{l=1}^{j-1} \sum_{m=0}^{k} \zeta_{l,k-m}\tau_{j-l,m}$$
$$+ \frac{1}{2}\sum_{l=0}^{k-1} \sum_{m=0}^{l} (\zeta_{k-l,l-m}\tau_{j+k-l,m} + \zeta_{j+k-l,m}\tau_{k-l,l-m}), \quad j = 1,2,\ldots \text{ and } k = 0,1,\ldots; \tag{3.2k}$$

$$\sigma_{jk} = -2\kappa\zeta_{jk}. \tag{3.2l}$$

In the above expressions the summation is taken to be identically zero if the lower limit exceeds the upper. Equations (3.2a, b) were derived from equations (2.10a, b), (3.2c, d) from (2.11a, b), (3.2e, f) by combining (2.8b) and (2.4a, b) in (2.6), (3.2g, h) from (2.8b), (3.2j, k) from (2.8c) and (3.2l) from (2.9). This system of equations (3.2) is closed only when we define the parameter ϵ.

(a) *Verification and extension of Wilton's work*

To verify Wilton's work we simply let $\epsilon = a_1$. From equation (3.1a) we see that this is equivalent to taking

$$\alpha_{10} = 1, \quad \alpha_{1k} = 0, \quad k = 1,2,\ldots.$$

We then substitute this into equations (3.2) and solve. The following results, up to $O(a_1^5)$ are then obtained:

$$a_1 = a_1;$$
$$a_2 = \frac{(\kappa-2)}{(2\kappa-1)}a_1^2 - \frac{(30\kappa^3 - 71\kappa^2 + 17\kappa - 8)}{8(2\kappa-1)^3(3\kappa-1)}a_1^4 + O(a_1^6); \tag{3.3a}$$

$$a_3 = \frac{9(2\kappa^2-11\kappa+8)}{16(2\kappa-1)(3\kappa-1)}a_1^3$$
$$-\frac{3(13248\kappa^5-53640\kappa^4+63260\kappa^3-29010\kappa^2+7971\kappa-1216)}{768(2\kappa-1)^3(3\kappa-1)^2(4\kappa-1)}a_1^5+O(a_1^7); \quad (3.3b)$$

$$a_4 = \frac{(18\kappa^3-183\kappa^2+361\kappa-128)}{12(2\kappa-1)(3\kappa-1)(4\kappa-1)}a_1^4+O(a_1^6); \quad (3.3c)$$

$$a_5 = \frac{25(288\kappa^5-4680\kappa^4+18980\kappa^3-24786\kappa^2+11091\kappa-1600)}{1536(2\kappa-1)^2(3\kappa-1)(4\kappa-1)(5\kappa-1)}a_1^5+O(a_1^7); \quad (3.3d)$$

$$K = 1+\kappa-\frac{(2\kappa^2-15\kappa+16)}{8(2\kappa-1)}a_1^2$$
$$+\frac{(24\kappa^5+220\kappa^4-2422\kappa^3+4701\kappa^2-2858\kappa+704)}{128(2\kappa-1)^3(3\kappa-1)}a_1^4+O(a_1^6); \quad (3.3e)$$

$$c^2 = 1+\kappa-\frac{(2\kappa^2+\kappa+8)}{8(2\kappa-1)}a_1^2$$
$$+\frac{(24\kappa^5-164\kappa^4-566\kappa^3+1821\kappa^2-1322\kappa+448)}{128(2\kappa-1)^3(3\kappa-1)}a_1^4+O(a_1^6). \quad (3.3f)$$

Equations (3.3*a–f*) agree with Wilton's equations (10)–(15) respectively, with due regard paid to changes in notation. We note the presence of singularities at

$$\kappa = \tfrac{1}{2}, \tfrac{1}{3}, \ldots,$$

equivalent to wavelengths of 2·44, 2·99 cm for water. This phenomenon is due to the primary wave undergoing a resonant interaction with one of its harmonics. The case $\kappa = \frac{1}{2}$ will be considered in greater detail in a later paper.

In theory we can carry on and find more coefficients (with the aid of a computer). However Schwartz showed for pure gravity waves that the coefficient a_1 is not a monotonically increasing function of the wave height. Instead he uses $\epsilon = h$ where h, the wave amplitude, is defined as

$$h = \tfrac{1}{2}(\eta_{\text{crest}}-\eta_{\text{trough}}).$$

Using (2.4*b*), this can be written as

$$h = \sum_{k=1}^{\infty}\frac{a_{2k-1}}{(2k-1)},$$

or, using equation (3.1*a*), as

$$h = \sum_{k=1}^{\infty}\Delta_k\epsilon^{2k-1}, \quad (3.4)$$

where

$$\Delta_k = \sum_{j=1}^{k}\frac{\alpha_{2j-1,k-j}}{(2j-1)}, \quad k = 1,2,\ldots, \quad (3.5)$$

so

$$\Delta_1 = 1, \quad \Delta_k = 0, \quad k = 2,3,\ldots, \quad (3.6)$$

in order that $\epsilon = h$. We then use this form of ϵ, in case a_1 is not monotonic in h for all values of κ. Also h is a more practical parameter to use and the trouble of calculating the amplitude in terms of a_1, at each step of the working, is removed.

In order to obtain the solution to high order, we programmed equations (3.2) together with the closure equations (3.6) in FORTRAN IV on Cambridge University's IBM 370/165 computer. The execution time for a quadruple precision (32 decimal places) solution up to $O(h^{100})$ was approximately 10 minutes and was independent of the input value of κ (which must be chosen initially). More coefficients are difficult to obtain owing to storage problems associated with quadruple precision arithmetic. A double precision (16 decimal places) run produced more coefficients but serious rounding error was evident in the higher-order terms. This choice, of fewer (more accurate) coefficients, turns out to be vindicated because the expansions (3·1) converge rapidly for particular values of κ. Consequently the higher-order terms are not as essential as may at first seem the case.

Runs were made with $\kappa = 0$, 0·000075, 0·0075, 0·8, 1·0, 5·0, 10·0. Other runs, with values of κ nearer to 0·5, were also made but the analysis of these is to be included in a subsequent paper. The case $\kappa = 0{\cdot}000075$ (a wavelength in water of approximately 200 cm) is not strictly suitable for inclusion as the effects of the air above could well have as comparable effect on the wave form as does surface tension. However it is instructive to compare it with the cases $\kappa = 0$ and 0·0075.

In addition the following results were obtained, for general κ, by hand:

$$a_1 = h - \frac{3(2\kappa^2-11\kappa+8)}{16(2\kappa-1)(3\kappa-1)}h^3 + O(h^5); \tag{3.7a}$$

$$a_2 = \frac{(\kappa-2)}{(2\kappa-1)}h^2 - \frac{(12\kappa^4-66\kappa^3+154\kappa^2-169\kappa+40)}{8(2\kappa-1)^3(3\kappa-1)}h^4 + O(h^6); \tag{3.7b}$$

$$a_3 = \frac{9(2\kappa^2-11\kappa+8)}{16(2\kappa-1)(3\kappa-1)}h^3 + O(h^5); \tag{3.7c}$$

$$a_4 = \frac{(18\kappa^3-183\kappa^2+361\kappa-128)}{12(2\kappa-1)(3\kappa-1)(4\kappa-1)}h^4 + O(h^6); \tag{3.7d}$$

$$a_5 = \frac{25(288\kappa^5-4680\kappa^4+18980\kappa^3-24786\kappa^2+11091\kappa-1600)}{1536(2\kappa-1)^2(3\kappa-1)(4\kappa-1)(5\kappa-1)}h^5 + O(h^7); \tag{3.7e}$$

$$\begin{aligned} K = 1+\kappa &- \frac{(2\kappa^2-15\kappa+16)}{8(2\kappa-1)}h^2 \\ &+ \frac{(72\kappa^5-428\kappa^4+446\kappa^3-129\kappa^2+454\kappa-64)}{128(2\kappa-1)^3(3\kappa-1)}h^4 + O(h^6); \end{aligned} \tag{3.7f}$$

$$\begin{aligned} c^2 = 1+\kappa &- \frac{(2\kappa^2+\kappa+8)}{8(2\kappa-1)}h^2 \\ &+ \frac{(72\kappa^5-428\kappa^4-194\kappa^3+735\kappa^2-74\kappa+64)}{128(2\kappa-1)^3(3\kappa-1)}h^4 + O(h^6). \end{aligned} \tag{3.7g}$$

The computed results for a particular value of κ agree exactly with those of equations (3.7), up to the orders given. In addition equations (3.7) can be shown to agree with Schwartz (1974) when $\kappa = 0$ and Crapper (1957) when κ is infinite.

(b) *Integral properties*

We can now draw wave profiles, using the a_n ($n = 1, 2, \ldots$) and equations (2.4a, b). However we can do more with the computed coefficients. In particular we can calculate phase speeds, kinetic and potential energies and mass, energy and momentum fluxes. For example the phase speed is given by equation (3.1g) and we calculate the required coefficients γ_n from equation (3.2a). To find the potential energy V, either we choose a_0 so that the mean level $\bar{\eta}$ vanishes or we can let $a_0 = 0$ and use equation (3.12a), below. We choose the latter. Other properties are found as follows. From equation (2.7) of I we have that

$$T = \frac{c}{4\pi}\int \eta(d\Phi + c\,dx) = \tfrac{1}{2}c^2\bar{\eta}. \tag{3.8}$$

In addition, letting $y \to -\infty$ in equation (2.3) of the present paper gives us

$$\bar{\eta} = \tfrac{1}{2}(K - c^2). \tag{3.9}$$

Hence

$$T = \tfrac{1}{4}c^2(K - c^2) \tag{3.10}$$

and

$$I = \tfrac{1}{2}c(K - c^2) \tag{3.11}$$

where, in (3.11), we have used the well-known result $2T = cI$ (see Longuet-Higgins (1975) for a proof in the case of pure gravity waves which can easily be extended to include gravity–capillary waves). With a non-zero mean level the potential energy V is given by

$$V = \tfrac{1}{2}(\overline{\eta^2} - \bar{\eta}^2) + \kappa[\overline{(1+\eta'^2)^{\frac{1}{2}} - 1}] \tag{3.12a}$$

$$= V_g + V_\tau \tag{3.12b}$$

(compare this with equation (2.3) of I). We can now greatly simplify V_τ as follows:

$$\begin{aligned}
\frac{V_\tau}{\kappa} + 1 &= \frac{1}{2\pi}\int_0^{2\pi} (1+\eta'^2)^{\frac{1}{2}}\,dx \\
&= \frac{1}{2\pi}\int_0^{2\pi c} (x_\Phi^2 + \eta_\Phi^2)^{\frac{1}{2}}\,d\Phi \\
&= \frac{1}{2\pi c}\int_0^{2\pi c} \left(\sum_{n=0}^{\infty} u_n \cos\left(\frac{n\Phi}{c}\right)\right) d\Phi \\
&= \frac{1}{2\pi c}\sum_{n=0}^{\infty} u_n \left[\int_0^{2\pi c} \cos\left(\frac{n\Phi}{c}\right) d\Phi\right] \\
&= u_0.
\end{aligned}$$

Note we have taken the positive root of $(1+\eta'^2)^{\frac{1}{2}}$ so as to be consistent with I. Then using (3.1e) and the fact that $\tau_{00} = 1$ [from (3.2e) with $k = 0$ and (3.2c)] we have

$$V_\tau = \kappa \sum_{k=1}^{\infty} \tau_{0k} h^{2k}, \tag{3.13}$$

V_g is given in terms of α_{ij} by Cokelet (1977), equations (5.23) and (5.24). This enables us to write

$$V_g = \frac{1}{4}\sum_{j=1}^{\infty}\sum_{k=0}^{j-1}\sum_{l=0}^{j-k-1}\frac{\alpha_{j-k-l,k}\,\alpha_{j-k-l,l}}{(j-k-l)^2}h^{2j}$$
$$+\frac{1}{8}\sum_{j=2}^{\infty}\sum_{m=1}^{j-1}\sum_{k=0}^{j-m-1}\sum_{i=0}^{j-m-k-1}\sum_{n=0}^{j-m-k-i-1}\left(\frac{1}{m}+\frac{2}{j-k-i-n}\right)$$
$$\times\frac{\alpha_{j-m-k-i-n,k}\,\alpha_{mi}\,\alpha_{j-k-i-n,n}}{(j-m-k-i-n)}h^{2j}$$
$$-\frac{1}{8}\sum_{j=2}^{\infty}\left\{\sum_{i=1}^{j-1}\left(\sum_{k=0}^{i-1}\sum_{n=0}^{i-k-1}\frac{\alpha_{i-k-n,k}\,\alpha_{i-k-n,n}}{(i-k-n)}\right)\right.$$
$$\left.\times\left(\sum_{l=0}^{j-i-1}\sum_{m=0}^{j-i-l-1}\frac{\alpha_{j-i-l-m,l}\,\alpha_{j-i-l-m,m}}{(j-i-l-m)}\right)\right\}h^{2j}. \quad (3.14)$$

Similarly using (3.1g) and (3.1h) we have

$$T = \frac{1}{4}\sum_{k=1}^{\infty}\sum_{l=1}^{k}(\delta_l-\gamma_l)\,\gamma_{k-l}\,h^{2k}. \quad (3.15)$$

For the radiation stress S_{xx} and energy flux F we use equations (2.23) and (2.24) of I viz.

$$S_{xx} = 4T-3V_g-V_\tau, \quad (3.16)$$

$$F = (3T-2V_g)\,c. \quad (3.17)$$

Crapper (1979) has given an expression for S_{zz}, the excess flux of z momentum in the z direction (where the z axis is such as to form a right-handed triad with the present (x, y) axes, that is, it is directed at right angles into the page). It is

$$S_{zz} = T-V_g-V_\tau. \quad (3.18)$$

The following expressions were then obtained:

$$T = \tfrac{1}{4}(1+\kappa)\,h^2+\frac{(-6\kappa^4+12\kappa^3-21\kappa^2+15\kappa)}{16(2\kappa-1)^2(3\kappa-1)}h^4+O(h^6); \quad (3.19)$$

$$V = \tfrac{1}{4}(1+\kappa)\,h^2+\frac{(-12\kappa^4+44\kappa^3-39\kappa^2+21\kappa+8)}{64(2\kappa-1)^2(3\kappa-1)}h^4+O(h^6); \quad (3.20)$$

$$S_{xx} = \tfrac{1}{4}(1+3\kappa)\,h^2+\frac{(-84\kappa^4+172\kappa^3-193\kappa^2+175\kappa-24)}{64(2\kappa-1)^2(3\kappa-1)}h^4+O(h^6); \quad (3.21)$$

$$S_{zz} = \frac{-(2\kappa^2+\kappa+8)}{64(2\kappa-1)}h^4+O(h^6); \quad (3.22)$$

$$F/c = \tfrac{1}{4}(1+3\kappa)\,h^2+\frac{(-18\kappa^4+42\kappa^3-37\kappa^2+34\kappa-4)}{16(2\kappa-1)^2(3\kappa-1)}h^4+O(h^6). \quad (3.23)$$

Equations (3.19) and (3.20) agree with deep-water linear theory, as do (3.21), (3.22) [see Longuet-Higgins & Stewart (1964), § 3, equations (6) and (23), respectively] and (3.23) [see Wehausen & Laitone (1960), equation (15.25)]. These results also agree with the known results for the limiting cases $\kappa = 0$ and κ infinite. Three other features of these equations are noted also. Firstly, the singularities at $\kappa = \frac{1}{2}, \frac{1}{3}, \ldots$ are still present. Secondly, $T - V$ $(= S_{zz})$ is positive if $\kappa < \frac{1}{2}$, and negative if $\kappa > \frac{1}{2}$ and we shall see that $V > T$ is characteristic of all capillary waves with $\kappa > \frac{1}{2}$ (we already know this when κ is infinite, see I, figure 2). Finally the order h^4 term in T vanishes at $\kappa = 0$ *and* at $\kappa = 1$, the other two roots being complex.

To conclude this section we note that when the expansion parameter was chosen to be the same as the one used by Cokelet (1977), namely

$$\epsilon^2 = \epsilon_c^2 = 1 - \frac{q_{\text{crest}}^2 \, q_{\text{trough}}^2}{c^4},$$

where q_{crest}, q_{trough} denote the particle speeds at the wave crest and wave trough respectively, several of the coefficients α_{ij}, β_{ij}, etc. are (for all h) complex-valued for $\kappa > \frac{1}{2}$. Of course this parameter is not necessarily applicable here. Its main merit, for pure gravity waves, is that it has a known range, viz. $0 \leqslant \epsilon_c \leqslant 1$. This is because q_{crest} was postulated, by Stokes, to have the value zero at the highest wave (in a reference frame moving with the wave crests). However on including surface tension, a sharp crest must be ruled out, on intuitive grounds at least. It can also be ruled out by using methods similar to those in § 4 of Schwartz (1974) to show that q_{crest} can never vanish. So, even if the α_{ij} etc. were not complex-valued we still would not know the range of ϵ_c *a priori*.

4. Results

Now we present wave profiles and integral properties of waves for various values of κ. It is to be noted that taking $\tau = 0$ (in the dimensional form of κ) is equivalent to taking λ infinite. In that sense, pure gravity waves will be included in the section on gravity waves together with $\kappa = 0{\cdot}000075$ and $\kappa = 0{\cdot}0075$. In the same sense pure capillary waves ($g = 0$) will be included under capillary waves, along with $\kappa = 0{\cdot}8$, $1{\cdot}0$, $5{\cdot}0$ and $10{\cdot}0$. The main results are plotted in figures 1–21 and tabulated (where appropriate) in the appendix. All the graphs were drawn with [13/13] Padé approximants and the tables contain these values, except for values of h near the highest, where the converged results are used. The values given are correct to the number of figures shown.

(*a*) *Gravity waves*

Work on pure gravity waves was verified. In particular tables 1 and 2 of Schwartz (1974), table 2 of Longuet-Higgins (1975), figures 19 and 20 and table A0 of Cokelet (1977) were all reproduced. Minor differences were encountered at heights very near to the maximum, owing to the fewer number of terms being used.

In the cases $\kappa = 0{\cdot}000075$ and $\kappa = 0{\cdot}0075$ we have now to consider what we shall call the highest wave. We have already excluded as a possibility the case of a sharp corner in the profile and, for these gravity waves, a criterion based on an enclosed bubble of air is obviously inapplicable. Another possible criterion, namely that the horizontal particle velocity (in the frame moving with the waves) should vanish somewhere in the profile implies that some part of the wave profile must be vertical and we shall see that this cannot be attained by our method. In our case we adopt the following criterion. Having solved (3.2) with (3.6) for the α_{ij}, we can then calculate

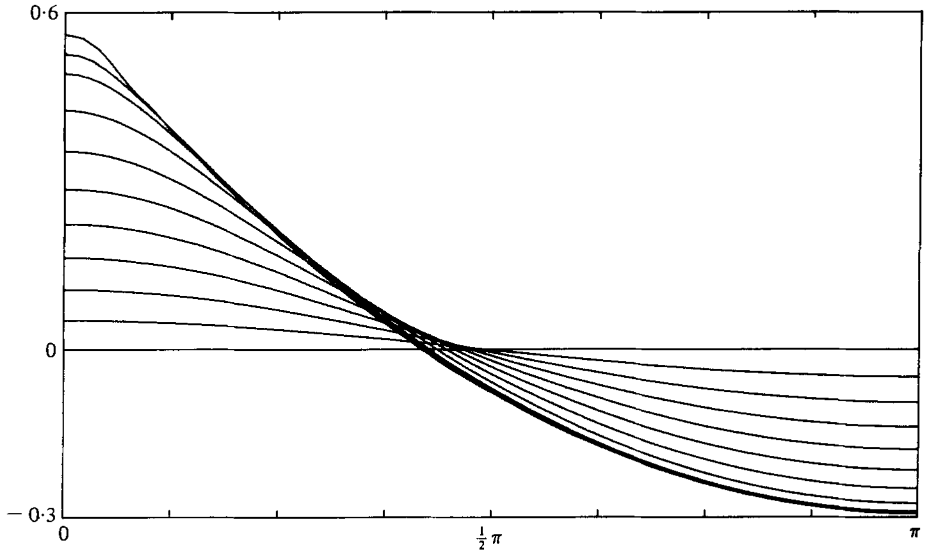

FIGURE 1. Wave profiles, in the case $\kappa = 0{\cdot}000075$, for $h = 0{\cdot}05$, $0{\cdot}10$, $0{\cdot}15$, $0{\cdot}20$, $0{\cdot}25$, $0{\cdot}30$, $0{\cdot}35$, $0{\cdot}39$, $0{\cdot}41$, $0{\cdot}43$. The still water line is included for reference.

a_i from (3.1a), with the aid of Padé approximants. Then if we do not get convergence in the Padé approximants, we cannot draw the wave profile by using equations (2.4). It must be stressed that this limiting criterion is only technical; the author has not yet seen any physical significance in this choice. This method is also dependent on what we call convergent. However it seems obvious, for consistency, to choose that used by Cokelet. That is, for a given value of i, take, for each value of h,

$$C = \frac{\{[N/N]\,a_i - [N-1/N-1]\,a_i\}}{hi}.$$

Then let $N = 1, 2, \ldots$ until either $C \leqslant 10^{-5}$ or we run out of coefficients α_{ij} to approximate. If the former, we take $[N/N]\,a_i$ as our value for a_i and go on to consider a_{i+1}; if the latter, we take a_{i-1} as the largest usable coefficient.

In applying this limiting criterion with the convergence condition, it was found that not all the a_i diverged after a certain height was passed. Groups of a_i persisted in converging as h increased, with others diverging. So the maximum height $h_{\max}$ was taken as the highest value of h at which the first 60 Fourier coefficients converged. For $\kappa = 0{\cdot}000075$, $h_{\max} = 0{\cdot}4365$ and for $\kappa = 0{\cdot}0075$, $h_{\max} = 0{\cdot}3545$ by this method. So for $h = h_{\max} + 0{\cdot}0001$, one or more of the a_i ($i = 1, 2, \ldots, 60$) diverged.

Whether or not these *are* highest waves remains to be seen. However work in progress on values of the radius of curvature at points along the wave profile indicate that as h increases towards $h_{\max}$, the radius of curvature appears to approach a constant value dependent only on κ. More numerical accuracy is required to support this conclusion, but it now seems that the values of $h_{\max}$ quoted here do have some relevance.

Finally, in the case of the gravity waves considered here, it is possible that for $\kappa = 0{\cdot}0075$ the Fourier coefficient a_{133} can be unusually large (the same applies to

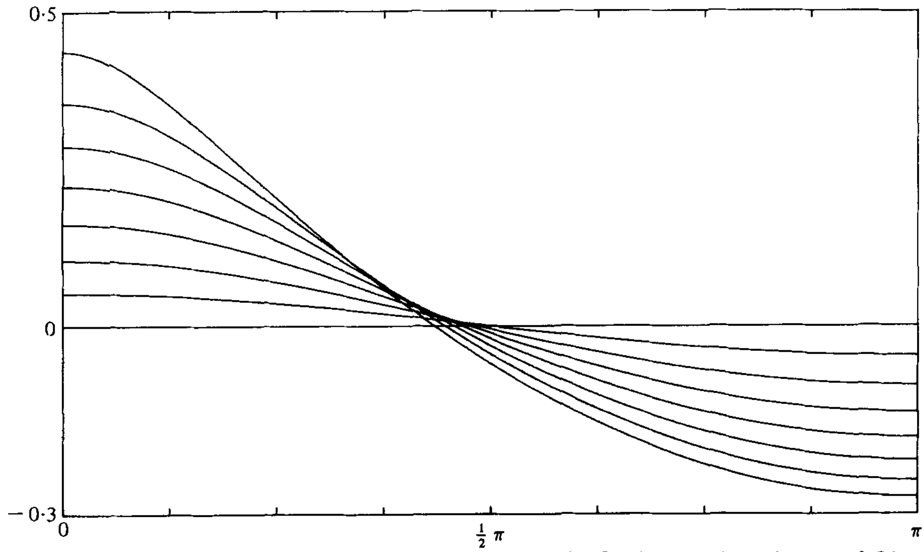

FIGURE 2. Wave profiles, in the case $\kappa = 0{\cdot}0075$, for $h = 0{\cdot}05$, $0{\cdot}10$, $0{\cdot}15$, $0{\cdot}20$, $0{\cdot}25$, $0{\cdot}30$, $0{\cdot}3545$. The still water line is included for reference.

$\kappa = 0{\cdot}000\,075$ and a_{13333}) owing to the denominator containing small terms ($133\kappa-1$ and $133\,33\kappa-1$ respectively). However it can be shown (for $\kappa = 0{\cdot}0075$) that $\alpha_{133,1} \doteqdot 10^{78}$, not too distant from the expected value of 10^{76}. (It is not possible, with present computer facilities, to find $\alpha_{13333,1}$ for $\kappa = 0{\cdot}000\,075$.) This is very close to the largest number that the computer can hold and is hence subject to serious rounding error. So the author tried out two other values of κ which would provide manageable coefficients, and give trouble at a_{80}. In each case ($\kappa = 199/16\,000$ and $399/32\,000$), the results for truncation at a_{72} and a_{100} were indistinguishable to 8 decimal places at $h_{\max}$ ($\doteqdot 0{\cdot}30$) in each case. Hence it seems that exclusion of these near-singular coefficients has no noticeable effect on our results.

In figure 1 we show wave profiles in the case $\kappa = 0{\cdot}000\,075$. Note (i) we do not draw the highest wave as the series in equations (2.4) do not converge well, as is the case for $\kappa = 0$ and $h = h_{\max} = 0{\cdot}44313$, (ii) the profile $h = 0{\cdot}43$ is almost entirely within the profile $h = 0{\cdot}41$, the former having a trough depth less than the latter and (iii) the profile $h = 0{\cdot}43$ has extra steepening just short of the crest, with a maximum local slope of $32{\cdot}6°$. In figure 2 with $\kappa = 0{\cdot}0075$ we have been able to draw the highest wave. The crest height and trough depth increase monotonically with h and the maximum wave slope is $20{\cdot}6°$. We note that no part of the wave profiles in either figure is vertical.

We now describe the behaviour of various integral properties of waves with $\kappa = 0{\cdot}000\,075$ and $0{\cdot}0075$ and compare them with pure gravity wave ($\kappa = 0$). First we consider the phase speed c. In figure 3 we have drawn $(c^2-c_0^2)/c_0^2$ against $h/h_{\max}$. c_0 is the phase speed of a wave of zero amplitude, given by $c_0^2 = 1+\kappa$. We note the presence of a maximum in each of the curves for $\kappa = 0$ (as found by Longuet-Higgins 1975) and $\kappa = 0{\cdot}000\,075$. Also the maximum value attained by $(c^2-c_0^2)/c_0^2$ for $\kappa = 0$ is larger than the maximum for $\kappa = 0{\cdot}000\,075$, but the value at $h = h_{\max}$ for $\kappa = 0$ is *lower* than

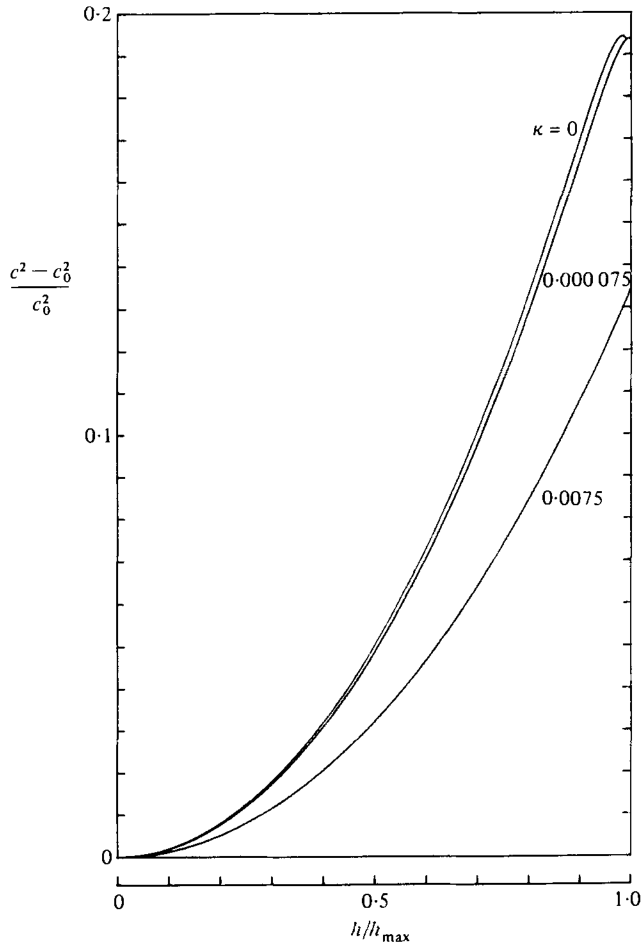

FIGURE 3

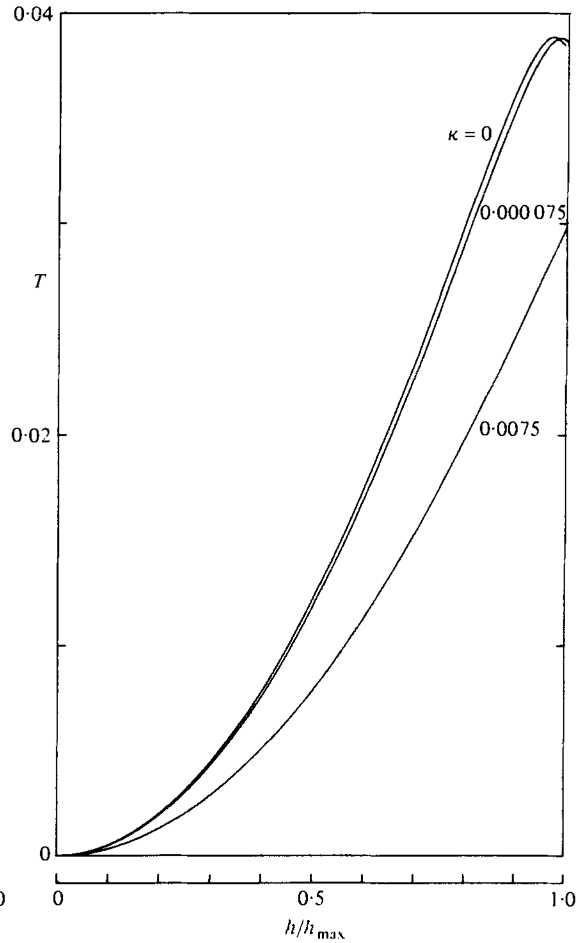

FIGURE 4

FIGURE 3. The relative increase in the squared phase speed c^2 to that of infinitesimal waves c_0^2, plotted against $h/h_{\max}$ for $\kappa = 0$, 0·000075, 0·0075.

FIGURE 4. The kinetic energy T plotted against $h/h_{\max}$ for $\kappa = 0$, 0·000075, 0·0075. The scaling is such that $g = 1$.

the corresponding value for $\kappa = 0{\cdot}000075$. In addition there is one point at which the curve for $\kappa = 0$ intersects with the curve for $\kappa = 0{\cdot}000075$.

In fact this sort of behaviour of these values of κ is typical of most of the wave properties. In figures 4 and 5 we plot the kinetic and potential energies of these waves against $h/h_{\max}$. From the tables we see that T is always greater than V. In figure 6 we plot V_τ against $h/h_{\max}$. The behaviour here is not typical but it is interesting to see how little of the potential energy is actually due to the stretching of the surface. In the case $\kappa = 0$, V_τ is identically zero. In figures 7 and 8 we plot S_{xx}, the excess flux of x momentum in the x direction, and S_{zz}, the excess flux of z momentum in the z direction, respectively, against $h/h_{\max}$. In figure 8 there is a maximum of S_{zz} in the case $\kappa = 0{\cdot}000075$ although this may not be obvious from the graph. Also, in figures 9 and 10

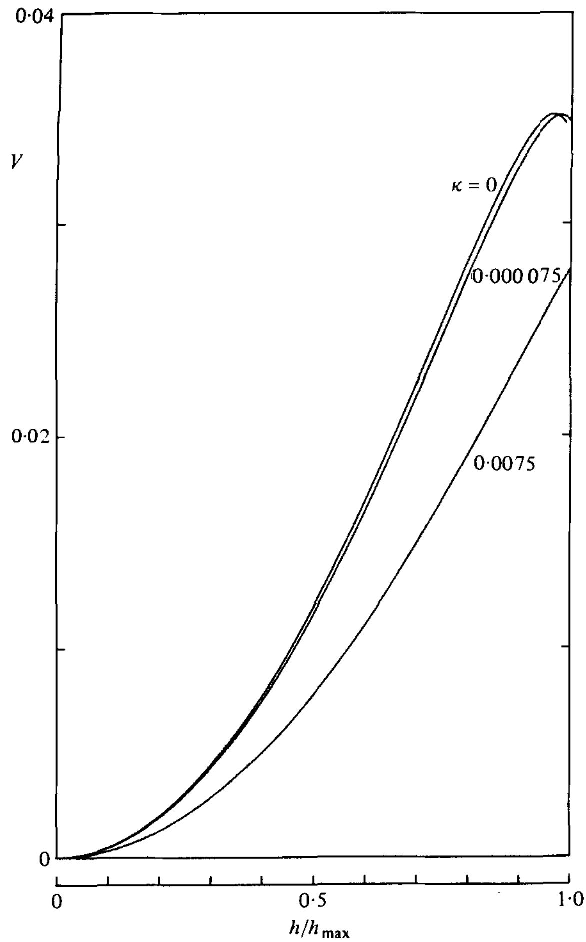

FIGURE 5. The potential energy V plotted against $h/h_{\max}$ for $\kappa = 0$, 0·000075, 0·0075. The scaling is such that $g = 1$.

we plot the fluxes of mass I and energy F, again, *versus* $h/h_{\max}$. The mean level $\bar{\eta}$ and Bernoulli constant exhibit similar behaviour and are not shown. $\bar{\eta}$ and V were checked, as in Cokelet (1977), by integration along the wave profile from their definitions. The intermediate maxima were confirmed and the deviation at most 2% (this occurred at $h = h_{\max}$).

Finally since the integral properties give us a hint as to its behaviour, we plotted a_1 against $h/h_{\max}$. For $\kappa = 0$ we know the behaviour is non-monotonic (Schwartz 1972) and now it comes as no surprise to find the same behaviour when $\kappa = 0{\cdot}000075$, see figure 11. In fact a_1 to a_{17} (for $\kappa = 0{\cdot}000075$) are non-monotonic in h (not shown). Note though that a_1 is monotonic in h when $\kappa = 0{\cdot}0075$ and this is reflected in the behaviour of its integral properties. Discussion of these results is delayed until § 5.

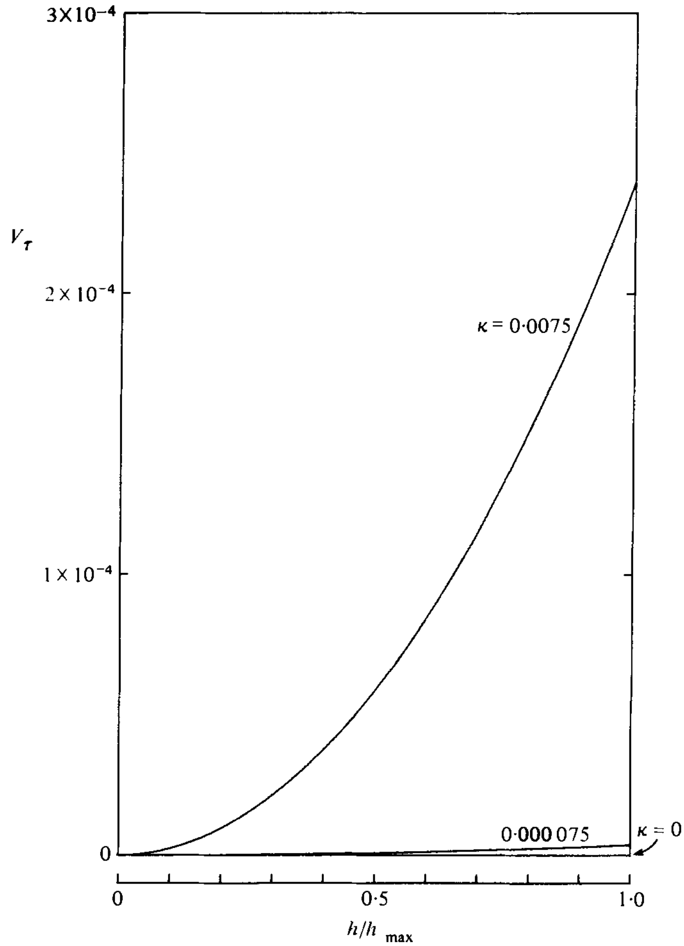

FIGURE 6. That part of the potential energy due to surface tension V_T plotted against h/h_{max} for $\kappa = 0$, 0·000075, 0·0075. The scaling is such that $g = 1$.

(*b*) *Capillary waves*

These waves are much easier to analyse and the convergence of all quantities in this section is remarkable. This is partly to be expected when one remembers the exact solution to the problem in the case $\kappa = \infty$ as given by Crapper (1957). However our method cannot deal with this case owing to the finite amount of computer storage available. But using Crapper's results and the results given in § 3 of I, we are able to compare large values of κ with the case $\kappa = \infty$. To do this requires a change in the scaling. Instead of $g = 1$, we take $\tau = 1$ so that (non-dimensional) $\kappa = 1/g$. Then the case $g = 0$ does correspond to the case $\kappa = \infty$.

Again we must answer the question: what is the highest wave? However this time the answer is much simpler. We have Crapper's criterion available, that is, the surface bends over and touches itself, enclosing a bubble of air. In fact we found this behaviour for $\kappa = 0·8$, 1·0, 5·0 and 10·0 and we obtained maximum heights by a simple technique,

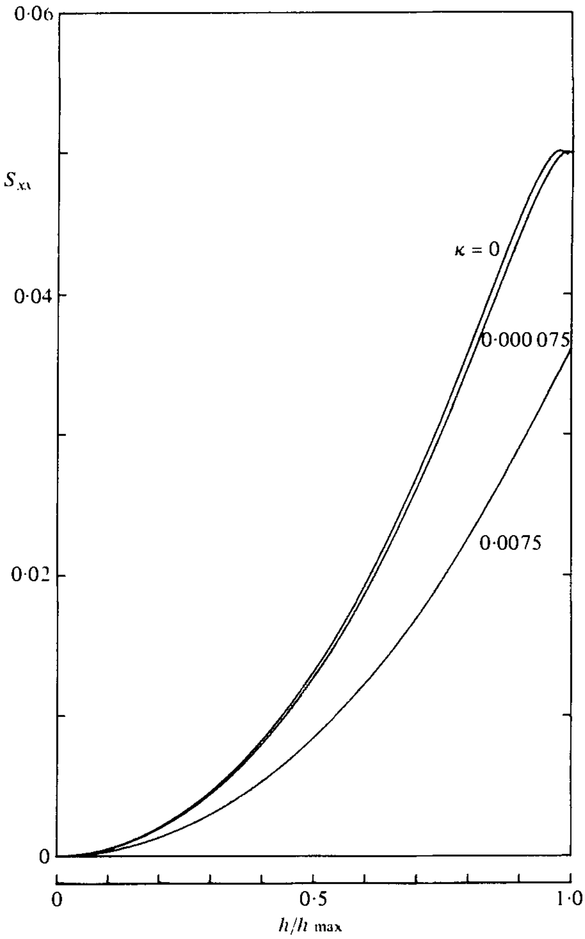

FIGURE 7

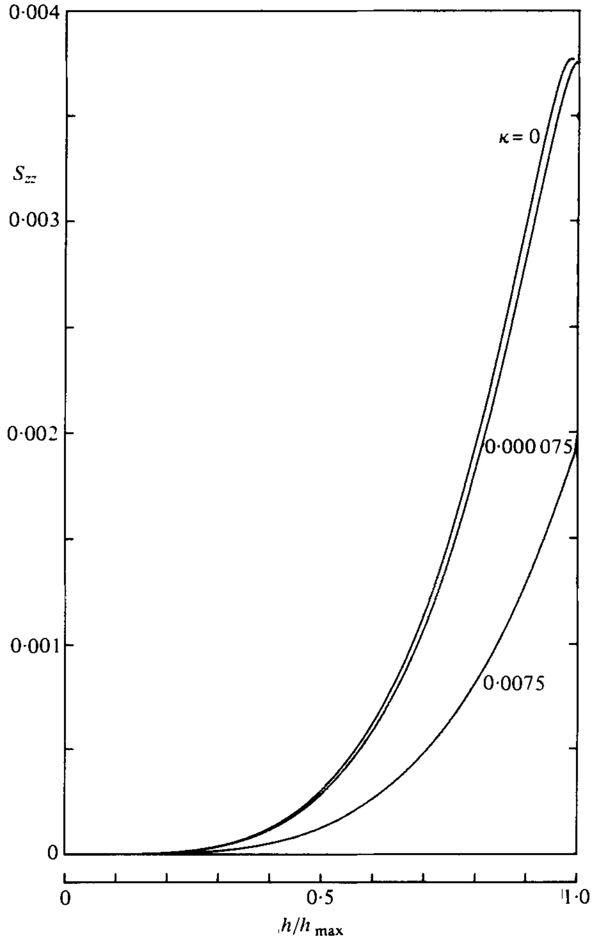

FIGURE 8

FIGURE 7. The radiation stress S_{xx} plotted against h/h_{max} for $\kappa = 0$, 0·000075, 0·0075. The scaling is such that $g = 1$.

FIGURE 8. The radiation stress, S_{zz}, plotted against h/h_{max} for $\kappa = 0$, 0·000075, 0·0075. The scaling is such that $g = 1$.

based on the method of interval halving, used in finding roots of polynomials. This implies that wave profiles could be drawn for $h > h_{max}$, but these profiles, of a very non-physical shape, can also be obtained from Crapper's solution. The values of h_{max} for various values of κ are given in table 1, where $\lambda = 2\pi$.

We have also drawn the highest wave profiles together (figure 12). The case $\kappa \doteq 0{\cdot}8$ is missing as it is very similar to the case $\kappa = 1{\cdot}0$. We note the dependence of trough depth and crest height on κ and the ever-present bubble. In the case $\kappa = 1{\cdot}0$, we have drawn profiles with h less than h_{max} as well as the highest; these are given in figure 13. Similar graphs can be drawn for $\kappa = 0{\cdot}8$, 5·0 and 10·0. Note that, as found in I for the case $\kappa = \infty$, the crest height above the mean level is not a monotonic function of wave amplitude.

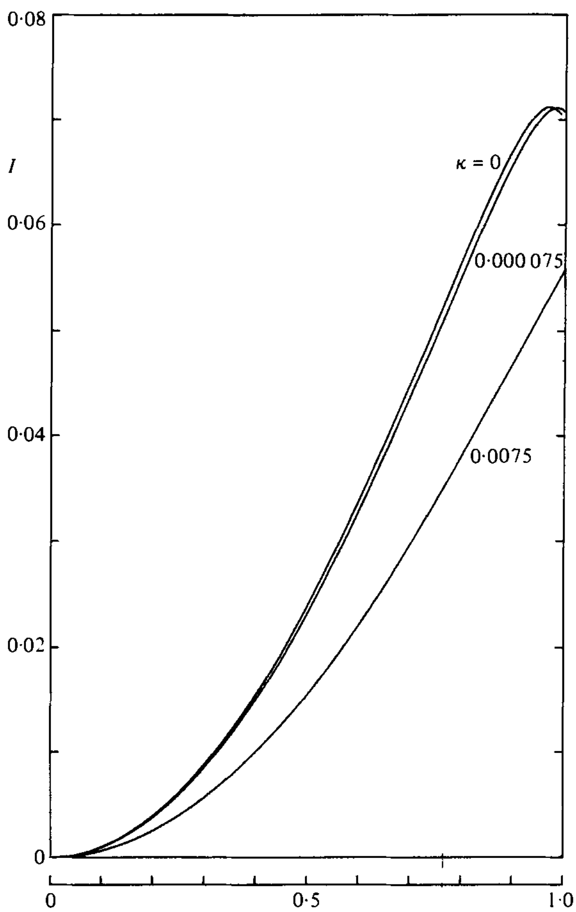

FIGURE 9

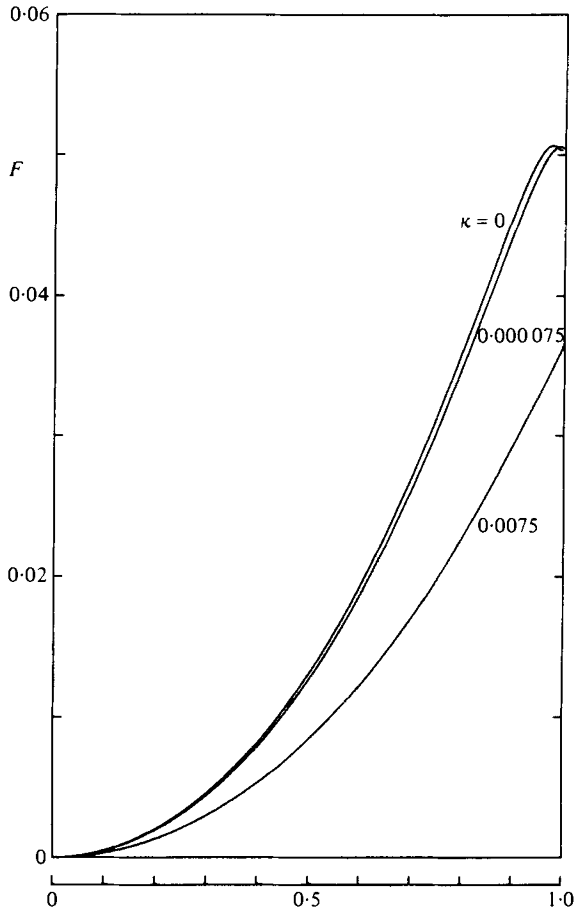

FIGURE 10

FIGURE 9. The wave momentum I plotted against h/h_{max} for $\kappa = 0$, 0·000075, 0·0075. The scaling is such that $g = 1$.

FIGURE 10. The energy flux F plotted against h/h_{max} for $\kappa = 0$, 0·000075, 0·0075. The scaling is such that $g = 1$.

The results for integral properties follow. In figure 14 we plot c^2/c_0^2 against h. Note that c^2/c_0^2 is a decreasing function of h for all values of κ and that the values of c^2/c_0^2 at $h = h_{max}$ decrease as κ decreases. In figure 15 we plot T against h/h_{max}. The curves for $\kappa = 1{\cdot}0$ and 0·8 possess maxima just short of $h = h_{max}$. In figure 16 we plot V against h/h_{max}. Here the behaviour is monotonic with h, but this covers up the rather interesting behaviour of V_g as given in figure 17. In each case of finite κ there is a well-defined maximum far short of $h = h_{max}$. Thus V_τ must rapidly increase beyond this maximum and this *is* the case as the surface starts to bend to enclose a bubble of air. We note that V_g for $\kappa = 1{\cdot}0$ appears greater for most of the range of h/h_{max} than V_g for $\kappa = 0{\cdot}8$. However the $\kappa = 0{\cdot}8$ curve represents a greater percentage of V_g in V than the $\kappa = 1{\cdot}0$, 5·0 and 10·0 curves for all values of h/h_{max}. As found in I for $\kappa = \infty$, we

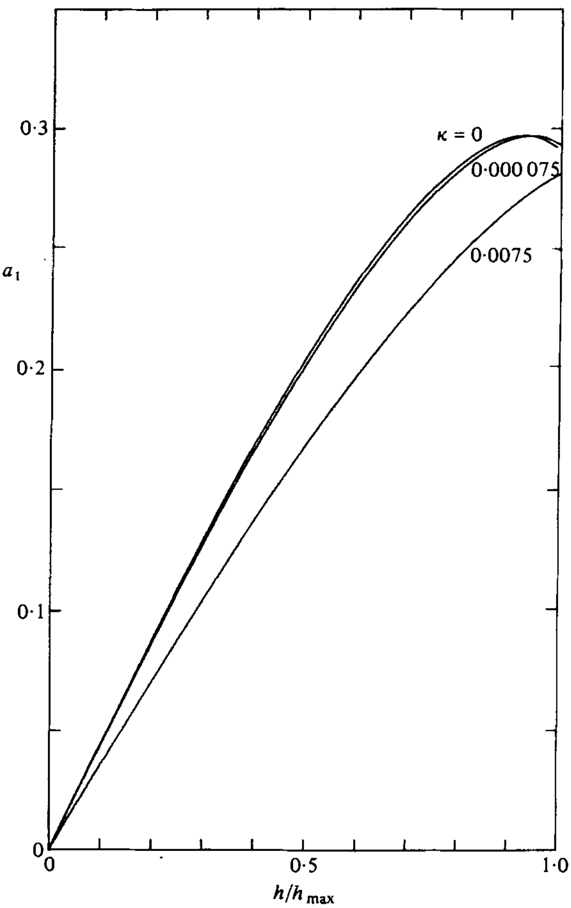

FIGURE 11. The leading Fourier coefficient of the wave profile, a_1, plotted against h/h_{max} for $\kappa = 0$, 0·000075, 0·0075.

κ	h_{max}
0	0·443 1
0·000 075	0·436 5
0·007 5	0·354 5
0·8	0·724 3
1·0	0·806 9
5·0	1·484 6
10·0	1·746 8
∞	2·292 6

TABLE 1. Highest waves for various values of κ.

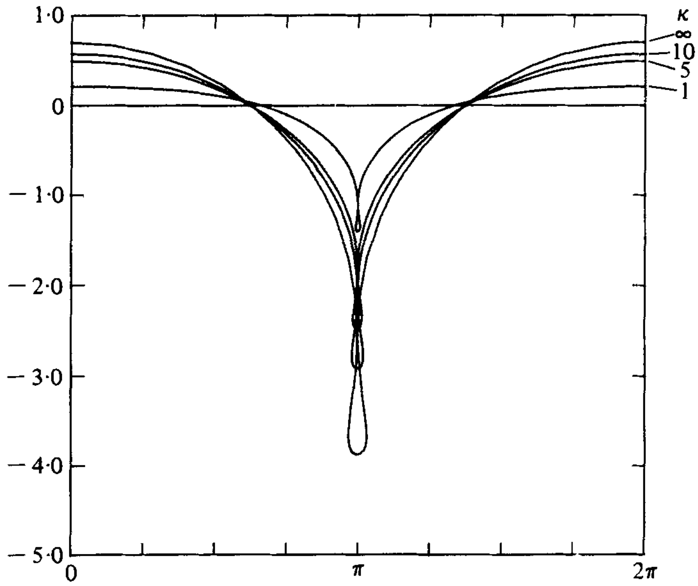

FIGURE 12. Highest wave profiles for $\kappa = 1, 5, 10, \infty$ drawn relative to the same mean level.

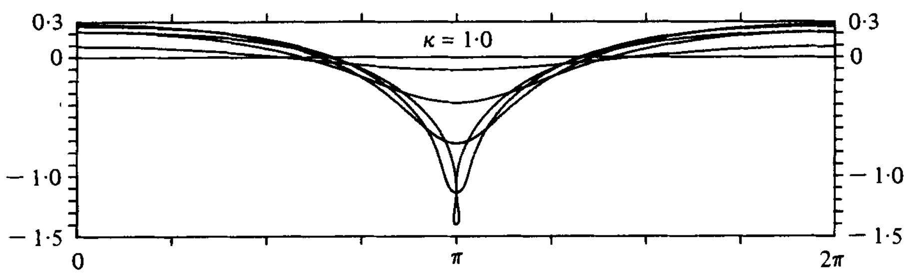

FIGURE 13. Wave profiles in the case $\kappa = 1{\cdot}0$ for $h = 0{\cdot}1, 0{\cdot}3, 0{\cdot}5, 0{\cdot}7, 0{\cdot}8069$. The still water line is included for reference.

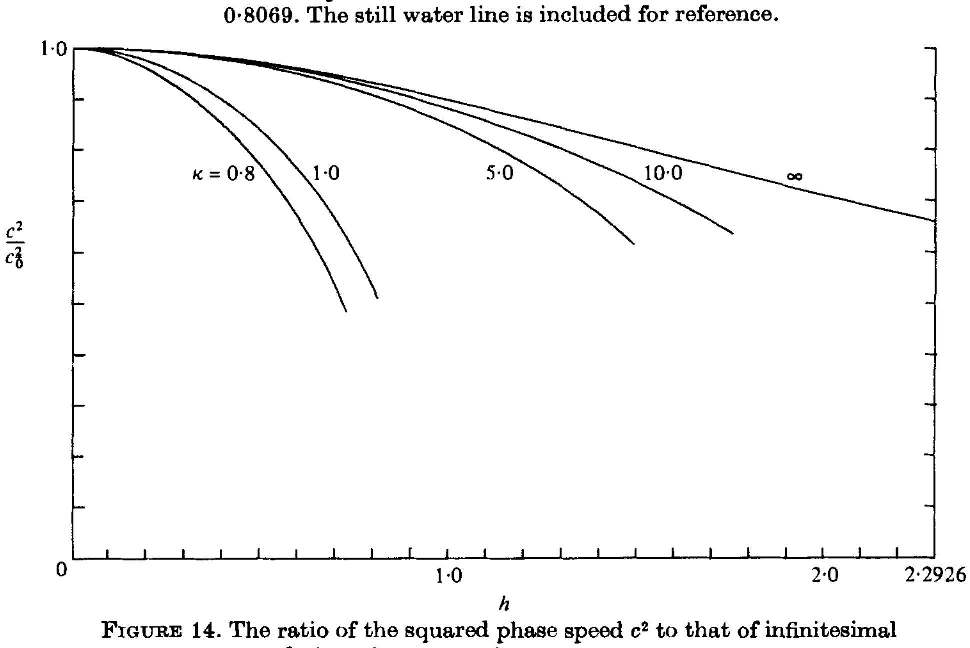

FIGURE 14. The ratio of the squared phase speed c^2 to that of infinitesimal waves c_0^2 plotted against h for $\kappa = 0{\cdot}8, 1{\cdot}0, 5{\cdot}0, 10{\cdot}0, \infty$.

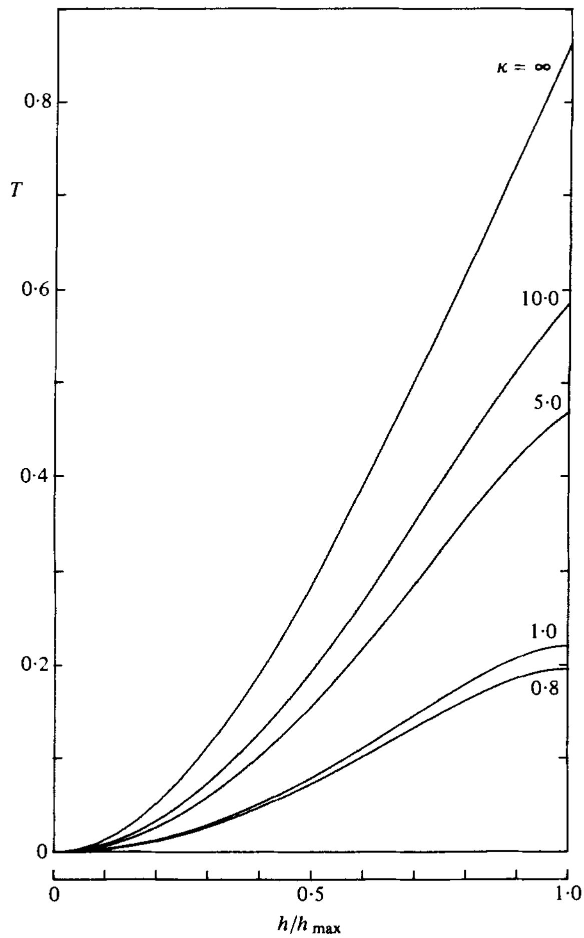

FIGURE 15

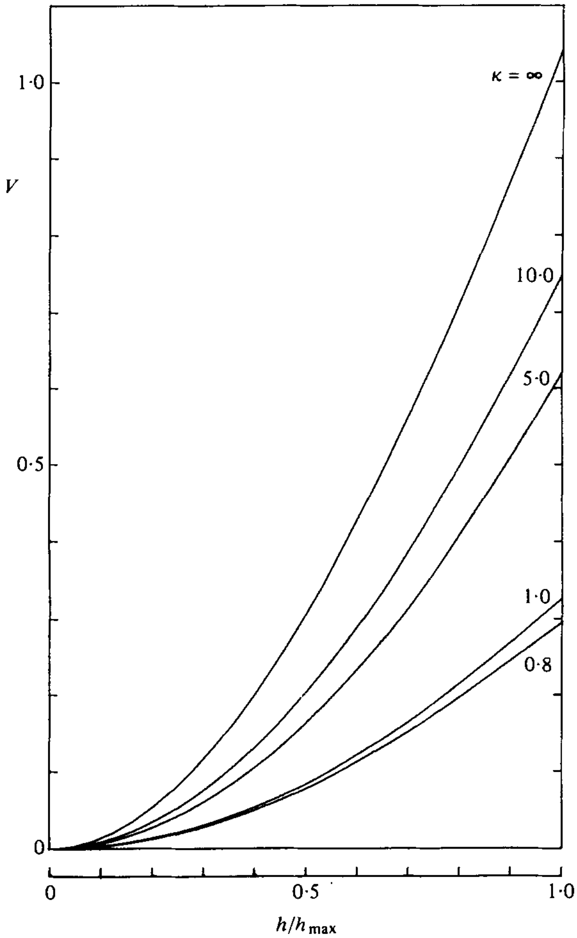

FIGURE 16

FIGURE 15. The kinetic energy T plotted against h/h_{max} for $\kappa = 0{\cdot}8, 1{\cdot}0, 5{\cdot}0, 10{\cdot}0, \infty$. The scaling is such that $\tau = 1$.

FIGURE 16. The potential energy V plotted against h/h_{max} for $\kappa = 0{\cdot}8, 1{\cdot}0, 5{\cdot}0, 10{\cdot}0, \infty$. The scaling is such that $\tau = 1$.

find here that V is always greater than T for given values of h and κ. In figure 18 we plot S_{xx} against h/h_{max}; non-monotonicity is absent. In figure 19 we plot S_{zz} against h/h_{max}. It will be noted that S_{zz} is always negative for non-zero h, indicating the flow of z momentum in the z direction for short waves is in the opposite direction to the case of long waves. In figure 20 and 21 we plot the fluxes of mass I and energy F. In the latter figure the curves $\kappa = 1{\cdot}0$ and $0{\cdot}8$ are non-monotonic. We note that the mean level and Bernoulli constant are monotonic in h. They are not shown. However table 2 contains values of η_{crest} and η_{trough} for various values of κ and h.

Finally we state that a_1 is also a monotonic function of h for the quoted values of κ. Hence we could have used it as an expansion parameter. In fact the whole analysis was repeated in this manner for the case $\kappa = 1{\cdot}0$ and six-figure accuracy retained

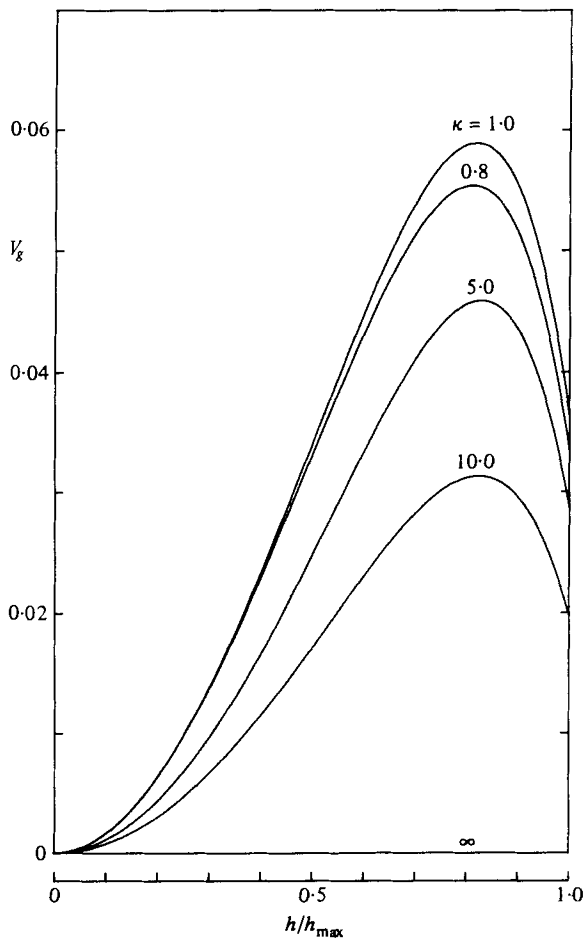

FIGURE 17

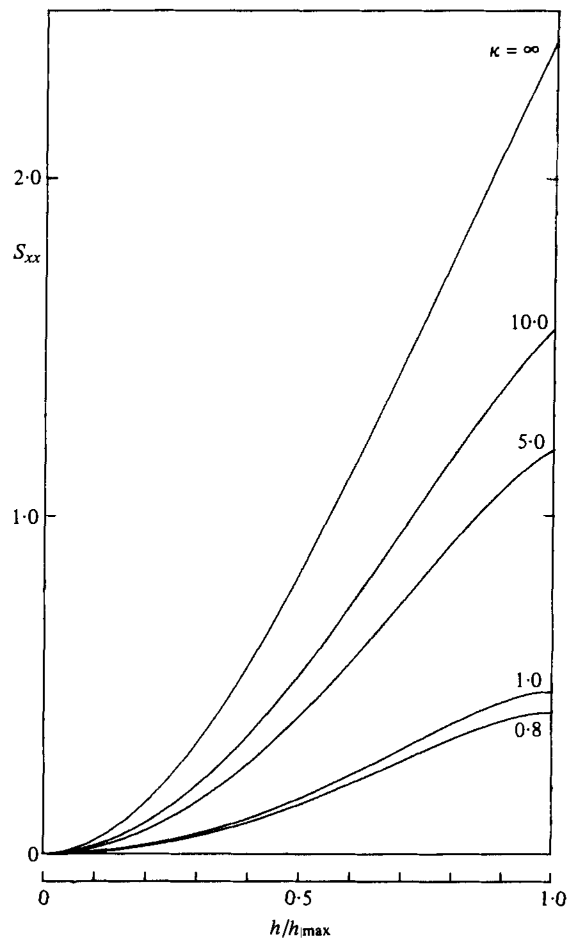

FIGURE 18

FIGURE 17. That part of the potential energy due to gravity V_g plotted against h/h_{max} for $\kappa = 0{\cdot}8$, $1{\cdot}0$, $5{\cdot}0$, $10{\cdot}0$, ∞. The scaling is such that $\tau = 1$.

FIGURE 18. The radiation stress S_{xx} plotted against h/h_{max} for $\kappa = 0{\cdot}8$, $1{\cdot}0$, $5{\cdot}0$, $10{\cdot}0$, ∞. The scaling is such that $\tau = 1$.

throughout, thus giving a check on the method. However when the mean level and potential energies were checked by the method of Cokelet (1977), severe disagreement was found in the case of the higher waves, for all values of κ. This was owing to the presence, in these waves, of two vertical tangents which the computer fails to represent accurately when integrating along the profile. Thus using a_1 as an expansion parameter was necessary if $\bar{\eta}$ and V were to be checked. The worst agreement was 0·001 %.

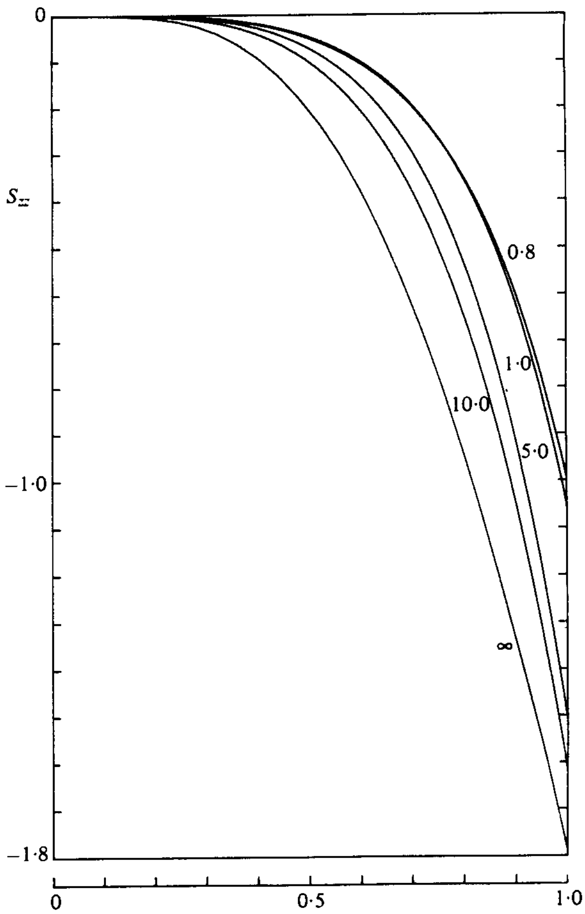

FIGURE 19

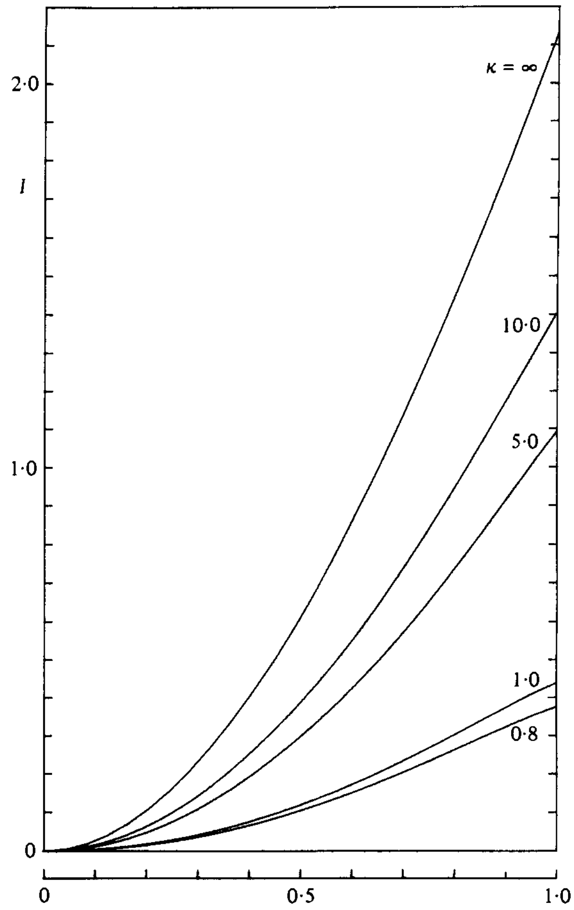

FIGURE 20

FIGURE 19. The radiation stress S_{zz} plotted against h/h_{max} for $\kappa = 0{\cdot}8,\ 1{\cdot}0,\ 5{\cdot}0,\ 10{\cdot}0,\ \infty$. The scaling is such that $\tau = 1$.

FIGURE 20. The wave momentum I plotted against h/h_{max} for $\kappa = 0{\cdot}8,\ 1{\cdot}0,\ 5{\cdot}0,\ 10{\cdot}0,\ \infty$. The scaling is such that $\tau = 1$.

5. Discussion

We have shown that gravity waves have non-monotonic integral properties even when there is a small amount of surface tension present. However, as we move to shorter waves, where surface tension dominates, the waves look and behave very much like pure capillary waves.

This work has implications for experimenters who seek non-monotonicity in gravity waves. For it now seems that they must deal with waves of substantial wavelengths if any progress is to be made. The author feels that if a wave of length less than 200 cm is looked at, the non-monotonic behaviour will be very hard to detect, as the maximum moves nearer to the line $h = h_{max}$. However, experimental work on

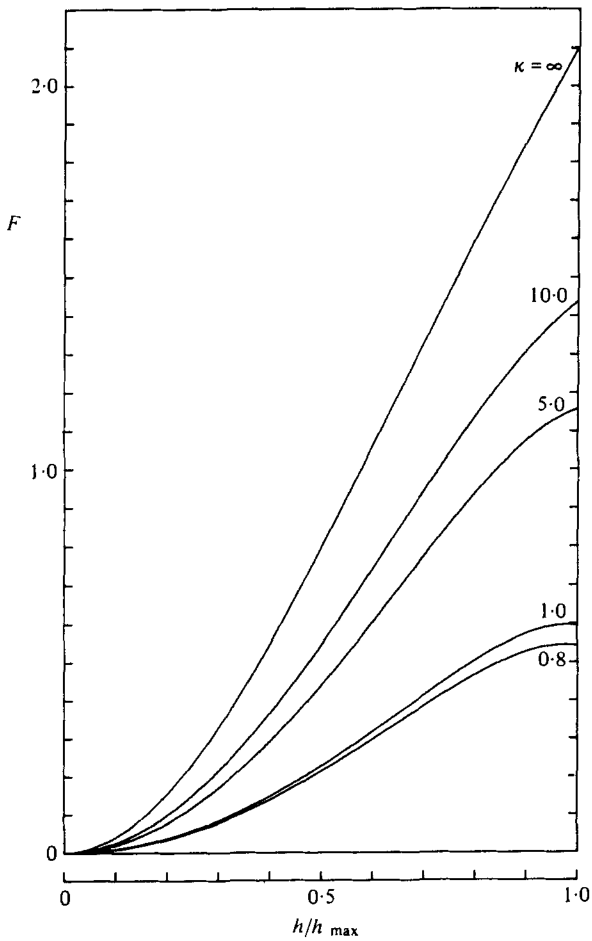

FIGURE 21. The energy flux F plotted against $h/h_{\max}$ for $\kappa = 0{\cdot}8$, $1{\cdot}0$, $5{\cdot}0$, $10{\cdot}0$, ∞. The scaling is such that $\tau = 1$.

capillary waves could produce the characteristic pure-capillary wave form because it now appears that waves of length 2 cm will have this form also. In practice viscosity will dampen the waves but not as fast as would be the case for waves of even shorter lengths.

In the case $\kappa = 0{\cdot}000075$ it should be possible to find instabilities in the manner of Longuet-Higgins (1978*a*, *b*). There, for pure gravity waves, evidence (both physical and numerical) was given as to the possibility of the maximum in the phase speed being responsible for the onset of an instability (it may also be instructive to apply the same methods to the case $\kappa = 0{\cdot}0075$ where no phase speed maximum is present). The work of Longuet-Higgins & Fox (1977, 1978) may also be adapted to see if the phase speed possesses any other extrema but there the difficulty will arise in defining accurately the highest wave. In addition this work can be extended to water of arbitrary uniform depth. Few wave profiles have been drawn by other authors for κ not equal to zero or infinity. Only Wilton's work is relevant and his profiles have been compared to Crapper's (see Wehausen & Laitone, 1960, p. 749). But as we pointed out at the end

$\kappa = 0{\cdot}000075$	h	0·1	0·2	C·3	0·35	0·39	0·41	0·43
	η_{crest}	0·105 069	0·221 164	0·351 687	0·425 053	0·490 300	0·526 1	0·561
	η_{trough}	−0·094 930	−0·178 834	−0·248 309	−0·274 946	−0·289 699	−0·293 4	−0·292
$\kappa = 0{\cdot}0075$	h	0·05	0·1	0·15	0·2	0·25	0·3	0·354 5
	η_{crest}	0·052 530	0·105 188	0·161 891	0·221 726	0·285 267	0·353 565	0·436 48
	η_{trough}	−0·047 470	−0·094 811	−0·138 107	−0·178 272	−0·214 730	−0·246 434	−0·272 59
$\kappa = 0{\cdot}8$	h	0·1	0·2	0·3	0·4	0·5	0·6	0·724 3
	η_{crest}	0·085 453	0·145 799	0·187 308	0·213 1	0·223 5	0·216 3	0·175
	η_{trough}	−0·114 546	−0·254 199	−0·412 688	−0·586 8	−0·776 7	−0·985 3	−1·280
$\kappa = 1{\cdot}0$	h	0·1	0·3	0·5	0·6	0·7	0·8	0·806 9
	η_{crest}	0·090 077	0·214 763	0·274 069	0·278 3	0·261 9	0·217 2	0·212 8
	η_{trough}	−0·109 923	−0·385 238	−0·726 025	−0·921 6	−1·138 1	−1·382 8	−1·401 1
$\kappa = 5{\cdot}0$	h	0·1	0·3	0·5	0·9	1·1	1·3	1·484 6
	η_{crest}	0·096 662	0·269 650	0·413 944	0·600 345	0·628 230	0·596 338	0·494 365
	η_{trough}	−0·103 338	−0·330 350	−0·586 056	−1·199 655	−1·571 769	−2·003 661	−2·474 834
$\kappa = 10{\cdot}0$	h	0·1	0·5	0·9	1·1	1·3	1·5	1·746 8
	η_{crest}	0·097 102	0·425 813	0·646 458	0·707 053	0·726 870	0·697 726	0·576 837
	η_{trough}	−0·102 898	−0·574 187	−1·153 542	−1·492 946	−1·873 129	−2·302 273	−2·916 762

TABLE 2. Results for η_{crest} and η_{trough} for various values of κ and h.

of § 4, because a_1 is monotonic in h, it is possible to extend Wilton's analysis to higher waves with the aid of Padé approximants.

Finally, we point out that an approach to the problem, based on $\eta = F(x)$ where F contains sines, cosines and their integral powers, will almost surely fail because as, we have shown, η is not always a single valued function of x.

In a subsequent paper the case of waves near to and at $\kappa = \frac{1}{2}$ will be analysed in detail. Consideration of the question of parasitic capillary waves is also delayed, possibly for inclusion in work where the full time-dependence of the problem is analysed.

While the final draft of this paper was being written, the author received preprints of papers by L. W. Schwartz & J.-M. Vanden-Broeck and B. Chen & P. G. Saffman. Both pairs of authors concentrate on the shorter waves, with the latter pair showing that bifurcations of the solution can exist. However neither paper gives details of integral properties, other than phase speeds.

Full details of the algorithm used to solve equations (3.2) are contained in the author's Ph.D. thesis (Hogan 1979*b*).

I would like to thank Professor M. S. Longuet-Higgins for suggesting this problem to me and the Natural Environment Research Council for financial support.

Appendix

h	c	T	V	V_τ	F	I	S_{xx}	S_{zz}
0	1·000 037 5	0	0	0	0	0	0	0
0·065 5	1·002 183 6	0·107 18 $\times 10^{-2}$	0·106 95 $\times 10^{-2}$	0·804 03 $\times 10^{-7}$	0·107 89 $\times 10^{-2}$	0·213 89 $\times 10^{-2}$	0·107 88 $\times 10^{-2}$	0·229 76 $\times 10^{-5}$
0·130 9	1·008 649 6	0·428 52 $\times 10^{-2}$	0·424 84 $\times 10^{-2}$	0·321 91 $\times 10^{-6}$	0·439 70 $\times 10^{-2}$	0·849 68 $\times 10^{-2}$	0·439 61 $\times 10^{-2}$	0·367 54 $\times 10^{-4}$
0·196 4	1·019 520 2	0·962 06 $\times 10^{-2}$	0·943 47 $\times 10^{-2}$	0·725 69 $\times 10^{-6}$	0·101 89 $\times 10^{-1}$	0·188 73 $\times 10^{-1}$	0·101 80 $\times 10^{-1}$	0·185 89 $\times 10^{-3}$
0·261 9	1·034 934 9	0·169 88 $\times 10^{-1}$	0·164 02 $\times 10^{-1}$	0·129 48 $\times 10^{-5}$	0·187 96 $\times 10^{-1}$	0·328 28 $\times 10^{-1}$	0·187 47 $\times 10^{-1}$	0·585 59 $\times 10^{-3}$
0·327 4	1·055 041 0	0·260 62 $\times 10^{-1}$	0·246 47 $\times 10^{-1}$	0·203 75 $\times 10^{-5}$	0·304 89 $\times 10^{-1}$	0·494 05 $\times 10^{-1}$	0·303 14 $\times 10^{-1}$	0·141 58 $\times 10^{-2}$
0·392 8	1·079 471 5	0·356 09 $\times 10^{-1}$	0·327 73 $\times 10^{-1}$	0·297 82 $\times 10^{-5}$	0·445 66 $\times 10^{-1}$	0·659 74 $\times 10^{-1}$	0·441 21 $\times 10^{-1}$	0·283 54 $\times 10^{-2}$
0·414 7	1·087 772 4	0·380 70 $\times 10^{-1}$	0·346 69 $\times 10^{-1}$	0·334 87 $\times 10^{-5}$	0·488 17 $\times 10^{-1}$	0·699 96 $\times 10^{-1}$	0·482 78 $\times 10^{-1}$	0·340 07 $\times 10^{-2}$
0·427 8	1·091 787	0·388 08 $\times 10^{-1}$	0·351 24 $\times 10^{-1}$	0·358 96 $\times 10^{-5}$	0·504 23 $\times 10^{-1}$	0·710 92 $\times 10^{-1}$	0·498 69 $\times 10^{-1}$	0·368 43 $\times 10^{-2}$
0·430 0	1·092 24	0·388 2 $\times 10^{-1}$	0·351 06 $\times 10^{-1}$	0·363 10 $\times 10^{-5}$	0·505 3 $\times 10^{-1}$	0·710 9 $\times 10^{-1}$	0·499 8 $\times 10^{-1}$	0·371 66 $\times 10^{-2}$
0·432 1	1·092 58	0·387 9 $\times 10^{-1}$	0·350 5 $\times 10^{-1}$	0·367 25 $\times 10^{-5}$	0·505 7 $\times 10^{-1}$	0·710 1 $\times 10^{-1}$	0·500 3 $\times 10^{-1}$	0·374 1 $\times 10^{-2}$
0·434 3	1·092 75	0·387 1 $\times 10^{-1}$	0·349 5 $\times 10^{-1}$	0·371 37 $\times 10^{-5}$	0·505 2 $\times 10^{-1}$	0·708 5 $\times 10^{-1}$	0·500 0 $\times 10^{-1}$	0·375 $\times 10^{-2}$
0·436 5	1·092 71	0·386 $\times 10^{-1}$	0·348 $\times 10^{-1}$	0·375 34 $\times 10^{-5}$	0·504 $\times 10^{-1}$	0·706 $\times 10^{-1}$	0·499 $\times 10^{-1}$	0·374 $\times 10^{-2}$

TABLE 3. Properties of the steady wave with $\kappa = 0{\cdot}000\,075$ as a function of the wave semi-height h. The scaling is such that $g = 1$.

h	c	T	V	V_τ	F	I	S_{xx}	S_{zz}
0	1·003 743 0	0	0	0	0	0	0	0
0·053 2	1·005 175 4	0·712 13 $\times 10^{-3}$	0·711 11 $\times 10^{-3}$	0·530 26 $\times 10^{-5}$	0·728 52 $\times 10^{-3}$	0·141 69 $\times 10^{-2}$	0·725 78 $\times 10^{-3}$	0·101 56 $\times 10^{-5}$
0·106 3	1·009 485 9	0·284 72 $\times 10^{-2}$	0·283 09 $\times 10^{-2}$	0·212 22 $\times 10^{-4}$	0·294 98 $\times 10^{-2}$	0·564 08 $\times 10^{-2}$	0·293 84 $\times 10^{-2}$	0·162 49 $\times 10^{-4}$
0·159 5	1·016 714 5	0·639 69 $\times 10^{-2}$	0·631 46 $\times 10^{-2}$	0·478 01 $\times 10^{-4}$	0·676 82 $\times 10^{-2}$	0·125 83 $\times 10^{-1}$	0·673 91 $\times 10^{-2}$	0·822 26 $\times 10^{-4}$
0·212 7	1·026 928 1	0·113 31 $\times 10^{-1}$	0·110 71 $\times 10^{-1}$	0·851 35 $\times 10^{-4}$	0·123 44 $\times 10^{-1}$	0·220 67 $\times 10^{-1}$	0·122 79 $\times 10^{-1}$	0·259 52 $\times 10^{-3}$
0·265 9	1·040 212 8	0·175 56 $\times 10^{-1}$	0·169 25 $\times 10^{-1}$	0·133 42 $\times 10^{-3}$	0·198 53 $\times 10^{-1}$	0·337 55 $\times 10^{-1}$	0·197 16 $\times 10^{-1}$	0·631 17 $\times 10^{-3}$
0·319 0	1·056 613 8	0·248 06 $\times 10^{-1}$	0·235 11 $\times 10^{-1}$	0·193 07 $\times 10^{-3}$	0·293 56 $\times 10^{-1}$	0·469 54 $\times 10^{-1}$	0·290 78 $\times 10^{-1}$	0·129 51 $\times 10^{-2}$
0·336 8	1·062 731 7	0·273 35 $\times 10^{-1}$	0·257 38 $\times 10^{-1}$	0·215 56 $\times 10^{-3}$	0·329 00 $\times 10^{-1}$	0·514 43 $\times 10^{-1}$	0·325 54 $\times 10^{-1}$	0·159 63 $\times 10^{-2}$
0·347 4	1·066 527	0·288 4 $\times 10^{-1}$	0·270 4 $\times 10^{-1}$	0·229 65 $\times 10^{-3}$	0·350 8 $\times 10^{-1}$	0·540 7 $\times 10^{-1}$	0·346 38 $\times 10^{-1}$	0·179 63 $\times 10^{-2}$
0·349 2	1·067 165	0·290 8 $\times 10^{-1}$	0·272 5 $\times 10^{-1}$	0·231 94 $\times 10^{-3}$	0·354 $\times 10^{-1}$	0·545 0 $\times 10^{-1}$	0·350 5 $\times 10^{-1}$	0·183 1 $\times 10^{-2}$
0·351 0	1·067 80	0·293 3 $\times 10^{-1}$	0·275 $\times 10^{-1}$	0·234 60 $\times 10^{-3}$	0·358 $\times 10^{-1}$	0·549 3 $\times 10^{-1}$	0·354 0 $\times 10^{-1}$	0·187 $\times 10^{-2}$
0·352 7	1·068 44	0·296 $\times 10^{-1}$	0·277 $\times 10^{-1}$	0·236 96 $\times 10^{-3}$	0·362 $\times 10^{-1}$	0·554 $\times 10^{-1}$	0·357 5 $\times 10^{-1}$	0·190 $\times 10^{-2}$
0·354 5	1·069 08	0·298 $\times 10^{-1}$	0·279 $\times 10^{-1}$	0·239 37 $\times 10^{-3}$	0·365 $\times 10^{-1}$	0·558 $\times 10^{-1}$	0·361 1 $\times 10^{-1}$	0·194 $\times 10^{-2}$

TABLE 4. Properties of the steady wave with $\kappa = 0{\cdot}0075$ as a function of the wave semi-height h. The scaling is such that $g = 1$.

h	c	T	V	V_g	F	I	S_{xx}	S_{zz}
0	1·500 000 0	0	0	0	0	0	0	0
0·108 6	1·489 939 0	0·667 64 × 10^{-2}	0·672 09 × 10^{-2}	0·361 56 × 10^{-2}	0·190 68 × 10^{-1}	0·896 19 × 10^{-2}	0·127 53 × 10^{-1}	−0·445 36 × 10^{-4}
0·217 3	1·461 901 4	0·267 95 × 10^{-1}	0·274 71 × 10^{-1}	0·136 46 × 10^{-1}	0·776 15 × 10^{-1}	0·366 58 × 10^{-1}	0·524 15 × 10^{-1}	−0·676 34 × 10^{-3}
0·325 9	1·418 359 9	0·594 40 × 10^{-1}	0·627 29 × 10^{-1}	0·279 20 × 10^{-1}	0·173 72	0·838 16 × 10^{-1}	0·119 19	−0·328 88 × 10^{-2}
0·434 6	1·358 337 0	0·101 67	0·111 97	0·431 03 × 10^{-1}	0·297 19	0·149 69	0·208 48	−0·103 08 × 10^{-1}
0·543 2	1·276 268 3	0·147 68	0·173 71	0·540 44 × 10^{-1}	0·427 47	0·231 42	0·308 90	−0·260 38 × 10^{-1}
0·651 9	1·158 472 5	0·186 06	0·244 99	0·515 70 × 10^{-1}	0·527 15	0·321 22	0·396 11	−0·589 30 × 10^{-1}
0·688 1	1·106 207 1	0·193 47	0·269 95	0·448 94 × 10^{-1}	0·542 71	0·349 78	0·414 11	−0·764 87 × 10^{-1}
0·709 8	1·070 142 7	0·195 60	0·284 97	0·387 02 × 10^{-1}	0·545 12	0·365 57	0·420 00	−0·893 78 × 10^{-1}
0·713 4	1·063 716 8	0·195 75	0·287 47	0·374 79 × 10^{-1}	0·544 92	0·368 05	0·420 54	−0·917 30 × 10^{-1}
0·717 1	1·057 159 5	0·195 83	0·289 97	0·361 96 × 10^{-1}	0·544 52	0·370 49	0·420 93	−0·941 45 × 10^{-1}
0·720 7	1·050 465 4	0·195 85	0·292 46	0·348 52 × 10^{-1}	0·543 94	0·372 88	0·421 17	−0·966 26 × 10^{-1}
0·724 3	1·043 628 3	0·195 79	0·294 95	0·334 43 × 10^{-1}	0·543 15	0·375 21	0·421 26	−0·991 74 × 10^{-1}

TABLE 5. Properties of the steady wave with $\kappa = 0·8$ as a function of the wave semi-height h. The scaling is such that $\tau = 1$.

h	c	T	V	V_g	F	I	S_{xx}	S_{zz}
0	1·414 213 6	0	0	0	0	0	0	0
0·121 0	1·407 122 2	0·732 25 × 10^{-2}	0·735 93 × 10^{-2}	0·360 59 × 10^{-2}	0·207 63 × 10^{-1}	0·104 08 × 10^{-1}	0·147 19 × 10^{-1}	−0·367 97 × 10^{-4}
0·242 1	1·386 064 1	0·291 71 × 10^{-1}	0·297 59 × 10^{-1}	0·137 65 × 10^{-1}	0·831 42 × 10^{-1}	0·420 92 × 10^{-1}	0·593 96 × 10^{-1}	−0·588 01 × 10^{-3}
0·363 1	1·350 880 5	0·646 94 × 10^{-1}	0·677 08 × 10^{-1}	0·285 73 × 10^{-1}	0·184 99	0·957 81 × 10^{-1}	0·133 92	−0·301 41 × 10^{-2}
0·484 1	1·299 521 3	0·111 30	0·121 20	0·447 95 × 10^{-1}	0·317 50	0·171 30	0·234 43	−0·989 63 × 10^{-2}
0·605 2	1·226 280 2	0·163 24	0·189 26	0·570 67 × 10^{-1}	0·460 56	0·266 23	0·349 55	−0·260 26 × 10^{-1}
0·726 2	1·117 674 2	0·208 14	0·269 23	0·553 92 × 10^{-1}	0·574 08	0·372 45	0·452 54	−0·610 91 × 10^{-1}
0·766 6	1·068 604 0	0·217 37	0·297 61	0·485 10 × 10^{-1}	0·593 16	0·406 82	0·474 84	−0·802 44 × 10^{-1}
0·790 8	1·034 503 9	0·220 35	0·314 80	0·419 65 × 10^{-1}	0·597 03	0·426 00	0·482 67	−0·944 54 × 10^{-1}
0·794 8	1·028 410 7	0·220 61	0·317 67	0·406 61 × 10^{-1}	0·597 01	0·429 04	0·483 46	−0·970 59 × 10^{-1}
0·798 8	1·022 188 4	0·220 80	0·320 54	0·392 90 × 10^{-1}	0·596 78	0·432 02	0·484 09	−0·997 38 × 10^{-1}
0·802 9	1·015 831 9	0·220 91	0·323 40	0·378 50 × 10^{-1}	0·596 33	0·434 94	0·484 54	−0·102 49
0·806 9	1·009 335 7	0·220 94	0·326 27	0·363 38 × 10^{-1}	0·595 65	0·437 79	0·484 81	−0·105 33

TABLE 6. Properties of the steady wave with $\kappa = 1·0$ as a function of the wave semi-height h. The scaling is such that $\tau = 1$.

h	c	T	V	V_g	F	I	S_{xx}	S_{zz}
0	1·095 445 1	0	0	0	0	0	0	0
0·222 7	1·091 468 2	$0·148\,04 \times 10^{-1}$	$0·148\,58 \times 10^{-1}$	$0·246\,10 \times 10^{-2}$	$0·431\,02 \times 10^{-1}$	$0·271\,27 \times 10^{-1}$	$0·394\,36 \times 10^{-1}$	$-0·540\,35 \times 10^{-4}$
0·445 4	1·079 335 5	$0·583\,25 \times 10^{-1}$	$0·592\,02 \times 10^{-1}$	$0·960\,33 \times 10^{-2}$	0·168 12	0·108 07	0·154 89	$-0·877\,00 \times 10^{-3}$
0·668 1	1·058 344 1	0·127 79	0·132 35	$0·205\,62 \times 10^{-1}$	0·362 21	0·241 49	0·337 68	$-0·456\,08 \times 10^{-2}$
0·890 8	1·026 973 1	0·218 09	0·233 15	$0·333\,65 \times 10^{-1}$	0·603 40	0·424 73	0·572 49	$-0·150\,62 \times 10^{-1}$
1·113 4	0·982 201 5	0·320 52	0·359 85	$0·438\,97 \times 10^{-1}$	0·858 22	0·652 66	0·834 44	$-0·393\,26 \times 10^{-1}$
1·336 1	0·917 904 3	0·419 39	0·509 48	$0·435\,74 \times 10^{-1}$	1·074 89	0·913 80	1·080 94	$-0·900\,89 \times 10^{-1}$
1·410 4	0·890 134 7	0·446 86	0·563 61	$0·382\,79 \times 10^{-1}$	1·125 16	1·004 03	1·147 28	−0·116 75
1·454 9	0·871 407 7	0·460 84	0·596 90	$0·331\,24 \times 10^{-1}$	1·147 00	1·057 68	1·180 20	−0·136 06
1·462 3	0·868 114 3	0·462 94	0·602 50	$0·320\,93 \times 10^{-1}$	1·149 93	1·066 54	1·185 07	−0·139 56
1·469 8	0·864 768 3	0·464 97	0·608 11	$0·310\,08 \times 10^{-1}$	1·152 63	1·075 35	1·189 74	−0·143 14
1·477 2	0·861 368 2	0·466 92	0·613 74	$0·298\,68 \times 10^{-1}$	1·155 12	1·084 14	1·194 21	−0·146 81
1·484 6	0·857 912 6	0·468 80	0·619 37	$0·286\,71 \times 10^{-1}$	1·157 37	1·092 88	1·198 48	−0·150 58

TABLE 7. Properties of the steady wave with $\kappa = 5·0$ as a function of the wave semi-height h. The scaling is such that $\tau = 1$.

h	c	T	V	V_g	F	I	S_{xx}	S_{zz}
0	1·048 808 8	0	0	0	0	0	0	0
0·262 0	1·044 128 4	$0·187\,40 \times 10^{-1}$	$0·188\,24 \times 10^{-1}$	$0·170\,41 \times 10^{-2}$	$0·551\,43 \times 10^{-1}$	$0·358\,97 \times 10^{-1}$	$0·527\,29 \times 10^{-1}$	$-0·840\,08 \times 10^{-4}$
0·524 0	1·030 229 0	$0·733\,26 \times 10^{-1}$	$0·746\,49 \times 10^{-1}$	$0·665\,35 \times 10^{-2}$	0·212 92	0·142 35	0·205 35	$-0·132\,32 \times 10^{-2}$
0·786 1	1·007 380 9	0·159 10	0·165 66	$0·142\,40 \times 10^{-1}$	0·452 12	0·315 86	0·442 24	$-0·656\,27 \times 10^{-2}$
1·048 1	0·975 580 3	0·268 78	0·289 15	$0·230\,37 \times 10^{-1}$	0·741 69	0·551 01	0·739 89	$-0·203\,71 \times 10^{-1}$
1·310 1	0·934 000 6	0·392 36	0·441 74	$0·300\,86 \times 10^{-1}$	1·043 21	0·840 18	1·067 54	$-0·493\,79 \times 10^{-1}$
1·572 1	0·880 227 6	0·515 56	0·619 27	$0·295\,56 \times 10^{-1}$	1·309 41	1·171 43	1·383 88	−0·103 71
1·659 5	0·858 782 0	0·552 97	0·683 06	$0·259\,60 \times 10^{-1}$	1·380 06	1·287 81	1·476 90	−0·130 09
1·711 9	0·844 862 8	0·573 75	0·722 26	$0·225\,66 \times 10^{-1}$	1·416 09	1·358 21	1·527 61	−0·148 51
1·720 6	0·842 458 6	0·577 07	0·728 86	$0·218\,95 \times 10^{-1}$	1·421 57	1·369 95	1·535 61	−0·151 79
1·729 3	0·840 029 2	0·580 33	0·735 47	$0·211\,92 \times 10^{-1}$	1·426 89	1·381 70	1·543 48	−0·155 13
1·738 1	0·837 574 2	0·583 55	0·742 09	$0·204\,56 \times 10^{-1}$	1·432 04	1·393 44	1·551 20	−0·158 54
1·746 8	0·835 092 9	0·586 72	0·748 74	$0·196\,86 \times 10^{-1}$	1·437 03	1·405 17	1·558 79	−0·162 01

TABLE 8. Properties of the steady wave with $\kappa = 10·0$ as a function of the wave semi-height h. The scaling is such that $\tau = 1$.

REFERENCES

COKELET, E. D. 1977 *Phil. Trans. Roy. Soc.* A **286**, 183–230.

CRAPPER, G. D. 1957 *J. Fluid Mech.* **2**, 532–540.

CRAPPER, G. D. 1979 *J. Fluid Mech.* **94**, 13–24.

HOGAN, S. J. 1979*a* *J. Fluid Mech.* **91**, 167–180.

HOGAN, S. J. 1979*b* Ph.D. Dissertation, Cambridge University.

LONGUET-HIGGINS, M. S. 1975 *Proc. Roy. Soc.* A **342**, 157–174.

LONGUET-HIGGINS, M. S. 1978*a* *Proc. Roy. Soc.* A **360**, 471–488.

LONGUET-HIGGINS, M. S. 1978*b* *Proc. Roy. Soc.* A **360**, 489–506.

LONGUET-HIGGINS, M. S. & FOX, M. J. H. 1977 *J. Fluid Mech.* **80**, 721–742.

LONGUET-HIGGINS, M. S. & FOX, M. J. H. 1978 *J. Fluid Mech.* **85**, 769–786.

LONGUET-HIGGINS, M. S. & STEWART, R. W. 1964 *Deep-Sea Res.* **11**, 529–562.

SCHWARTZ, L. W. 1972 Ph.D. Dissertation, Stanford University.

SCHWARTZ, L. W. 1974 *J. Fluid Mech.* **62**, 553–578.

STOKES, G. G. 1880 *Math. & Phys. Papers* **1**, 225–228.

WEHAUSEN, J. V. & LAITONE, E. V. 1960 *Encyclopaedia of Physics* (ed. S. Flügge), vol. **9**, pp. 446–778.

WILTON, J. R. 1915 *Phil. Mag.* **29** (6), 688–700.